Aus dem Institut für Prophylaxe und Epidemiologie der Kreislaufkrankheiten (IPEK)
Klinikum der Universität München, Ludwig-Maximilians-Universität München

Vorstand: Prof. Dr. med. Christian Weber

Thema der Dissertation

A microscopic and transcriptome sequencing approach to protective mechanisms of opioid receptor stimulation in murine pressure overload induced heart failure

Dissertation
zum Erwerb des Doktorgrades der Medizin an der Medizinischen Fakultät der
Ludwig-Maximilians-Universität zu München
vorgelegt von
Daniel Nils Deußen
aus
Mönchengladbach

2021

Mit Genehmigung der Medizinischen Fakultät der Universität München

Berichterstatter:	Prof. Dr. med. Reinhard Lorenz
Mitberichterstatter:	PD Dr. med. Simon Deseive
	Prof. Dr. Elisabeth Deindl
Dekan:	Prof. Dr.med. Thomas Gudermann
Tag der mündlichen Prüfung:	07.10.2021

Table of content

1. Abstract

Background:

Heart Failure (HF) is a major cause of morbidity and mortality worldwide. Decreased cardiac output and weakened contractile function are major factors accompanying disease progression in HF. This inefficiency leads to pathological remodeling that alters the functional and structural state of the myocardium. In contrast, exercise leads to physiological hypertrophy and remodeling that is beneficial to the heart leading to increased efficiency. In a model of pressure overload induced left ventricular hypertrophy we were able to show that opioid receptor agonists (ORA) are able to maintain heart function when compared to vehicle treated controls. We now aim to investigate the structural advantages of ORA treatment and the underlying cardio protective mechanisms.

Methods:

Transverse aortic constriction (TAC) or sham surgery was performed on male C57Bl/6J mice at 8-10 weeks of age. Echocardiography (ECHO) was utilized before surgery and biweekly at post TAC/sham to determine heart function and left ventricular dimensions. Two weeks after surgery the animals were randomly allocated to receive either vehicle control, an irreversible δ-opioid receptor agonist (FIT), or the selective κ-ORA (U50,488H). All three agents were administered intraperitoneally (FIT, 10µg/kg every 72h; U50488H, 1.25mg/kg or vehicle daily). At 10 weeks animals were scarified. Four to six hearts per group were prepared for histological and expression analysis and two hearts per group were perfused for transmission electron microscopy (TEM). RNA sequencing was utilized to compare RNA expression levels of the left ventricle between treatment groups.

Results:

The hypertrophic response to TAC surgery was not altered by any of the two ORA treatments. Microscopical analysis indicated less fibrosis and maintained structural integrity in κ-ORA treated TAC hearts. RNA sequencing analysis at study end point revealed altered apelin and HIF-1 signaling pathways after κ-ORA stimulation.

Conclusion:

Treatment with κ-ORA (U50.488H) might offer a novel therapeutic option to preserve heart function in pressure overload induced left ventricular hypertrophy. Results from RNA sequencing suggest that this protection may be mechanistically linked to apelin and HIF-1 signaling pathways.

2. Zusammenfassung

Hintergrund:
Herzversagen (HF) ist weltweit einer der häufigsten Gründe für Morbidität und Mortalität. Verminderte kardiale Pumpleistung und abnehmende Kontraktilität sind Hauptfaktoren, die zum Progress des HF führen. Diese Ineffizienz bedingt auch eine pathologische Umstrukturierung in Funktion und Aufbau des Myokards. Im Gegensatz dazu, führt die sportliche Beanspruchung des Herzens zu einer physiologischen Hypertrophie und zu einer gesteigerten Effizienz. In einem Model der Hochdruck induzierten linksventrikulären Hypertrophie, konnten wir zeigen, dass Opioid Rezeptor Agonisten (ORA) die Fähigkeit besitzen die Herzfunktion zu erhalten, im Vergleich zu Vehikel-behandelten Kontrollen. Unser Ziel ist nun die strukturellen Vorteile einer ORA Behandlung und die zugrunde liegenden protektiven Mechanismen zu erforschen.

Methoden:
Transverse Aortenkonstriktion (TAC) oder Sham Operationen wurden an 8-10 Wochen alten, männlichen C57Bl/6J Mäusen durchgeführt. Echokardiografie (ECHO) wurde vor der OP und dann zweiwöchentlich nach TAC/Sham durchgeführt, um die Herzfunktion und linksventrikuläre Dimensionen zu bestimmen. Zwei Wochen nach OP erhielten die Tiere entweder eine Vehikel Kontrolle, den irreversiblen δ-Opioid Rezeptor Agonisten (FIT), oder den selektiven κ-ORA (U50,488H). Alle drei Agentien wurden intraperitoneal injiziert (FIT, 10µg/kg alle 72h; U50488H, 1.25mg/kg und Vehikel täglich). Vier bis sechs Herzen pro Gruppe wurden für die Histologie- und Expressionsanalysen vorbereitet. Zwei Herzen pro Gruppe wurden für Transmissionselektronenmikroskopie (TEM) perfundiert. RNA Sequenzierung wurde genutzt, um die RNA Expression im linken Ventrikel zu bestimmen.

Ergebnisse:
Die hypertrophe Reaktion auf die TAC-OP wurde durch die zwei ORA nicht verhindert. Mikroskopische Analysen deuteten auf weniger Fibrose und eine erhaltene strukturelle Integrität der mit κ-ORA behandelten TAC Herzen hin. Die RNA Sequenzierung zum Studienendpunkt zeigte Veränderungen in Apelin und HIF-1 Signalwegen durch κ-ORA Stimulation.

Schlussfolgerung:
Die Behandlung mit κ-ORA (U50.488H) könnte eine neue therapeutische Option zum Erhalt der Herzfunktion in Bluthochdruck-bedingter linksventrikulärer Herzhypertrophie sein. Die Ergebnisse der RNA Sequenzierung ließen dabei die Verbindung der protektiven Wirkung der κ-ORA zu den Apelin und HIF-1 Signalwegen vermuten.

3. Introduction and Background

3.1. Cardiovascular disease and heart failure

Cardiovascular disease (CVD) is a major cause of morbidity and mortality in the developed world. With an increase of over 21 % in just one decade, by 2017 CVD attributed to 17.8 million deaths worldwide [1]. In Europe alone CVD cause four million deaths per year, and cost estimated 210 billion Euros per year for the EU's economies [2].

Heart failure can be the endpoint of different cardiovascular diseases and remains an increasing global health problem. The HF prevalence continued to rise from 5.7 million American adults (≥20 years of age) between 2009 and 2012 to 6.2 million between 2013 and 2016 [1]. The increase is especially found in geriatric populations and half of the patients who develop HF die within five years of diagnosis [3]. The estimated costs of heart failure in the United States are more than $30 billion each year which includes treatment, medication, healthcare services and missed days of work [4]. The aging global population will thus pose challenges for global healthcare [5].

The current HF definition limits itself to the stage of clinical symptoms [6]. A failing heart is incapable to maintain the demanded cardiac output, which ultimately leads to progressive organ failure and death. In the early stages of disease progression this often goes unnoticed by the patient. At this point structural changes to the myocardium are already established, with decreased force production, reduced vascularization and constrained energy supply [7] [8]. Initiating an early treatment here may reduce mortality in patients with asymptomatic systolic LV dysfunction [9]. However, physicians are frequently consulted much too late, after the patient's daily life becomes more and more impaired by the disease. The early limitations in patients' lives are fatigue and shortness of breath. Restrictions in everyday activities, such as grocery shopping, climbing stairs or even basic routines as walking, occur and worsen over time [6]. When heart failure manifests, main symptoms are a general feeling of fatigue or weakness in everyday life, shortness of breath when lying down, weight gain with swelling of the feet, legs, ankles, or stomach.

3.1.1. Heart failure classification

Heart failure is graded by the New York Heart Associations (NYHA) score.

Table 1: Heart failure NYHA classification (Content from Russell *et al.* 2009 [10]).

NYHA Class	Patient Symptoms
I	No limitation of physical activity. Ordinary physical activity does not cause undue fatigue, palpitation, dyspnea (shortness of breath).
II	Slight limitation of physical activity. Comfortable at rest. Ordinary physical activity results in fatigue, palpitation, dyspnea (shortness of breath).
III	Marked limitation of physical activity. Comfortable at rest. Less than ordinary activity causes fatigue, palpitation, or dyspnea.
IV	Unable to carry on any physical activity without discomfort. Symptoms of heart failure at rest. If any physical activity is undertaken, discomfort increases.

Class	Objective Assessment
A	No objective evidence of cardiovascular disease. No symptoms and no limitation in ordinary physical activity.
B	Objective evidence of minimal cardiovascular disease. Mild symptoms and slight limitation during ordinary activity. Comfortable at rest.
C	Objective evidence of moderately severe cardiovascular disease. Marked limitation in activity due to symptoms, even during less-than-ordinary activity. Comfortable only at rest.
D	Objective evidence of severe cardiovascular disease. Severe limitations. Experiences symptoms even while at rest.

3.1.2. Heart failure subgroups

In the recent years the definition of heart failure has evolved. The European Society of Cardiology states:
"Heart failure is a clinical syndrome in which patients have typical symptoms and signs resulting from an abnormality of cardiac structure and function" [11].
In the past, heart failure was defined as systolic dysfunction. At this point diastolic dysfunction was referred to as compensated heart hypertrophy. In recent years the terms heart failure with preserved ejection fraction (HFpEF) and heart failure with reduced ejection fraction (HFrEF) have been introduced. HFpEF is often referred to as diastolic heart failure. Here the heart contracts normally, but relaxation during diastole is impaired, leading to reduced filling of the ventricle. HFrEF or systolic HF shows impaired contractility of the ventricle, resulting in less oxygenated blood being pumped through the body. In an attempt to fill the gap between these two classifications, heart failure with mid-range ejection fraction (HFmrEF) has been introduced into the most recent "ESC Guidelines on Acute and Chronic Heart Failure". Several clinicians already suggested that HFrEF and HFmrEF are just different in severity but are the same disease. Webb *et al.* compared 677 patients according to the 2016 ESC guidelines, with best outcomes for patients with HFmrEF. This group showed fewer deaths than HFrEF and less frequent rehospitalization compared to HFpEF [12].
The upcoming years will have to show if the new classification remains relevant in the clinical setting. Especially the reproducibility and precision of echocardiography is important for appropriate classification and for guidance of further patient treatment.
HFrEF has been declining over the last years, mostly due to extensive use of re-vascularization techniques [13]. Further reasons for the alteration in HF disease occurrence, are therapeutic progress, risk factors and the age profile of patients. HFpEF risk factors mainly consist in older age, but further in obesity and hypertension. Nowadays HFpEF already accounts for more than half of the HF patients [14].

Initial epidemiological studies revealed the leading cause of left ventricular systolic dysfunction (LVSD) to be hypertension [15]. However, over the last four decades this has gradually transitioned to ischemic heart disease (IHD) [16].
The early derail of what the body asks for and what the heart is capable of delivering is usually not noticed by the individual. A slow decline in function goes often unobserved but shows already the molecular and metabolic pathology that will later determine a poor disease outcome. Early changes are detected on a molecular and mitochondrial level, that often don't show signs of an already manifesting pathology.

The body responds to down winding contractility with the activation of the sympathetic and RAAS system [17]. In the long run, this sympathetic activation leads to an elevated pressure-load and tachycardia, alongside with increased oxygen consumption. These sympathetic mechanisms are well tuned during short term challenges, stress adaptation and physical activity. But on the long run, a constant hyperactive state of the heart leads to exhaustion on a micro and macro level.

For the last decades, modulating the sympathetic activity and the RAAS-hyperactivity has been the key approach, trying to prevent disease progression and have in fact considerably improved survival. Figure 1 shows an overview of the RAAS-system and the most common treatment options in heart failure. For detailed reviews on the extensive field please refer to Rossignol *et al*. and Lang *et al.* [17 18].

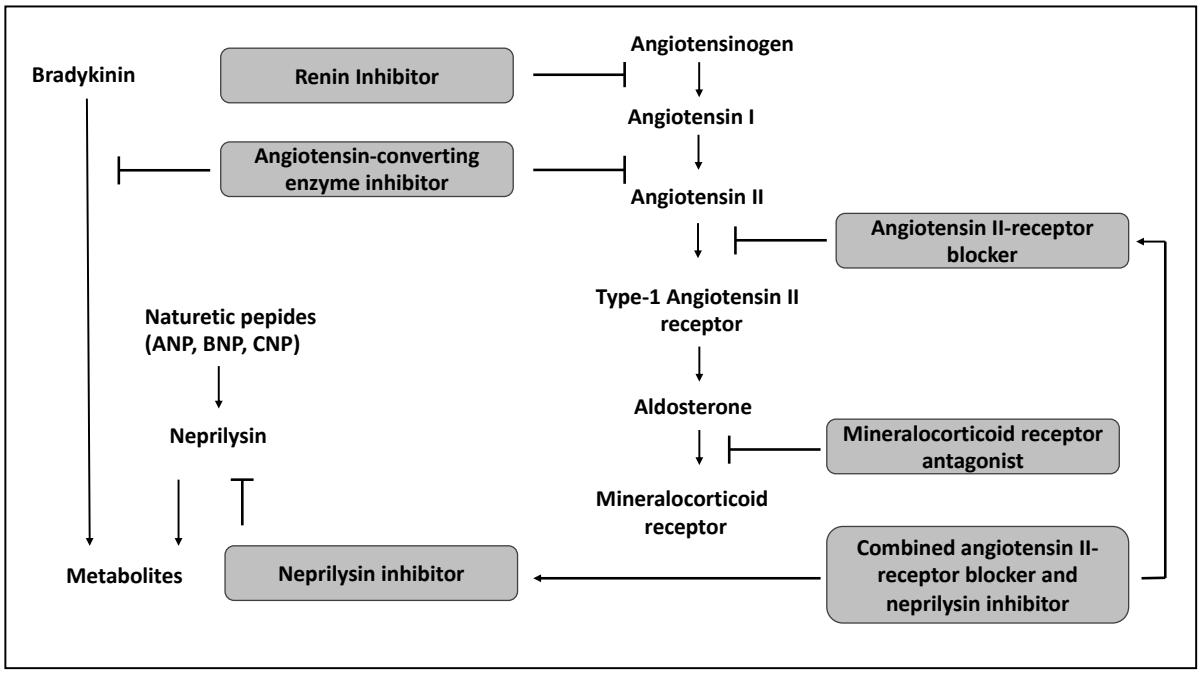

Figure 1: Overview of the RAAS-system and treatment options in HF. Figure by DN Deussen adapted from Lang *et al.* [18]

3.2. Cardiac hypertrophy

Hypertrophy is defined as a growth adaptation to a stimulus, when delivered performance does not meet the demands anymore. This can be due to increased requirements as in early development and growth, or during pregnancy, when the mother's heart has to supply two bodies. But it also includes states where we challenge our bodies and just perform longer, stronger or both. These above-mentioned processes of adaptation already show how complex and diverse cardiac hypertrophy is. In a growing child this

means increase in cell number as well as a gain in cell size. The cardiomyocyte turnover time in adulthood is low and adaptation is gained by an increase in dimension, rather than through the generation of new cells. Cardiac hypertrophy is accompanied by expansion of the capillary network to ensure sufficient nourishment. A tight connection between cell and vessel development is maintained in healthy individuals, and this perfect alignment guarantees function and organ nourishment [19].

Pathologic cardiac hypertrophy on the other hand is associated with a growth out of proportion. Hemodynamic-overload, increased levels of neurohumoral mediators, cell injury, reorganization and/or loss of cardiomyocytes can be observed [20]. Cardiomyocytes are able to detect changes in mechanical load and send out biochemical information about these changes. This phenomenon is called mechanotransduction and it gives the heart the capability to react to altered environmental conditions [21]. The heart is subjected to very different forces with each contractile movement. Stretch, shear stress and afterload challenge the myocardium, additionally the heart also obtains, integrates and sends information about the current circumstances [22]. The myocyte cytoskeleton is a very important sensor of mechanical stress and mediates the remodeling of the heart. Changes in cytoskeleton composition can be early signs of maladaptive remodeling. Recent findings also linked mechanotransduction during shear stress and/or stretch to altered mitochondrial metabolism, Ca^{2+} signaling and ionic homeostasis [23].

In both physiological state and in pathological remodeling, the interrelationship of prevalent pressure, volume and wall stress determine the heart's mechanics. Geometry and pressure changes are intertwined in their development and are used to predict the wall stress according to the law of Laplace [24].

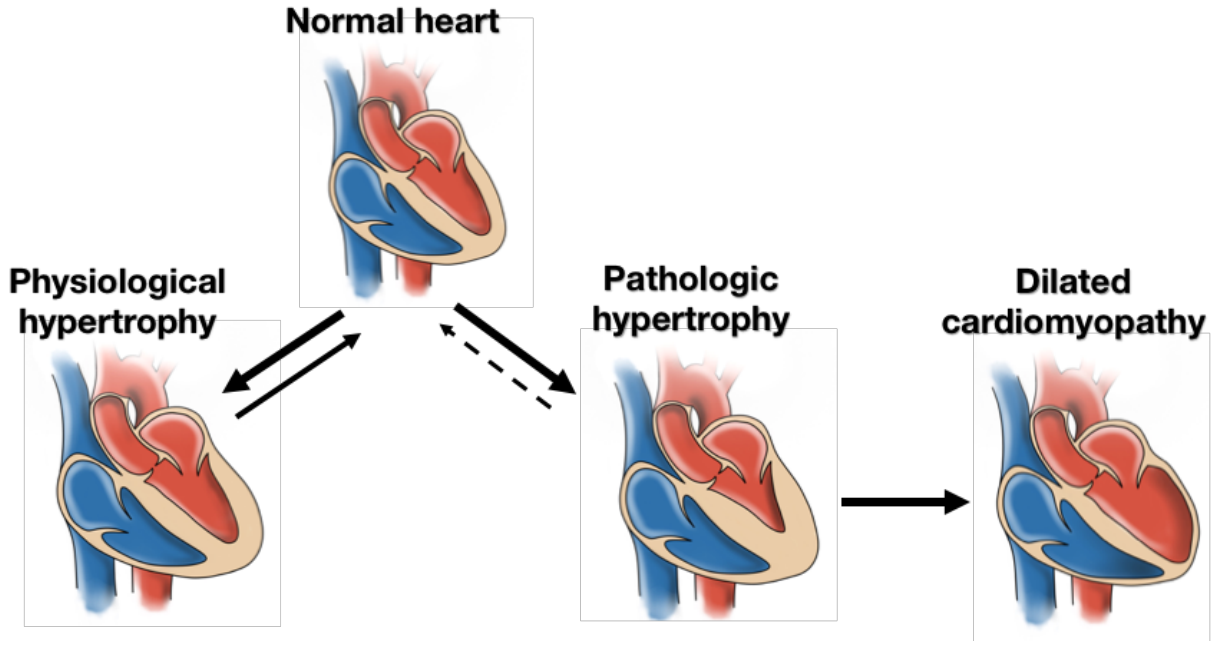

Figure 2: Left ventricular remodeling. Transition from a normal healthy heart towards A. a physiological adaptation and adequate hypertrophy to an external stimulus. This process seems to be reversible. B. a pathologic hypertrophy due to an insufficient cardiac output. Pathologic hypertrophy seems to be not fully reversible and has dangerous potential to progress into a dilated cardiomyopathy. By Huebner T & Deussen DN.

3.2.1. Myocardial hypertrophy in extreme settings

Observations in different athletic regimes have helped to understand that the outcome of an adaptive process is very much influenced by the trigger. An endurance athlete induces hypertrophy with a volume overload, which leads to eccentric cardiac hypertrophy. The main response of the heart here is a gain in output and this is achieved by an increase in longitudinal dimensions of the left ventricle. Accordingly, a thickening of the LV-wall and the septum, can be observed, with an augment in the myocyte length, increasing the overall LV volume [25]. When comparing stroke volume of untrained individuals during exercise to highly trained endurance athletes, only in athletes stroke volume can double from 80-135ml to more than 200ml [26] [27]. In disease, eccentric hypertrophy occurs in myocardial infarction and dilated cardiomyopathy and often establishes a ventricular dilatation.

Weightlifters and wrestlers expose their hearts to pressure overload, with peak pressures up to 320/250 mmHg, during their isometric exercise [28]. This leads to concentric hypertrophy with thickening of the LV with only minor dilatation of the ventricle. Concentric hypertrophy occurs when high, intermittent, maximal pressure forces challenge the heart.

Increased free wall and septal thickness with decreased ventricular volume can be seen in strength athletes. An augmented cell cross-section offers potential for greater generation of power, with increases rather in thickness, than in length [29]. Rising demands for higher pump forces in disease may result from valvular dysfunction or hypertension. The elevated force production attempts to maintain a sufficient ejection fraction in early disease development.
As a parade example, competitive rowing results in a combined phenotype of hypertrophy. The eccentric enlargement is thought to be due to the immense workload with extreme increase of cardiac output [30]. But rowing, with its heavy strength proportion, promotes concentric myocyte growth, too. The driver appears to be the contraction power that is needed to empty the enlarged chambers. Rowers and canoeists show the highest level of LV hypertrophy, with both thickened walls and enlarged ventricular cavity. Of the 16 thickest ventricles in the above-mentioned study, 15 belonged to rowers and canoeists, with greatest LV wall dimensions of 16mm, despite the generally low blood pressure in endurance athletes.

A very interesting type of cardiac adaptation can be observed during pregnancy. In the second and third trimester, more and more cardiac output is needed to ensure sufficient placental blood flow. Here again a volume overload leads to an eccentric cardiac hypertrophy [31]. As in de-training, pregnancy induced hypertrophy is fully reversible after child delivery, when the cardiac load returns to normal. Only a very small percentage of women develop a peripartum cardiomyopathy (PPCM) [32]. What makes the difference in this subgroup is still a topic in recent research. The 2015 Review of Bollen *et al.* discusses similarities and differences between PPCM and DCM. Both share common predisposing mutations, decreased vasculature and sarcomere integrity. But the authors speak of two different diseases in the clinic, with different pace in disease progression, outcome and underlying mechanisms [33].

3.2.2. Physiology vs. pathology

In the literature there is often a sharp distinction between physiological and pathological hypertrophy. This is of benefit, when we want to talk about the global differences, but overlap and get even misleading, when we go further into the details of similarities and differences. It is of importance to consider, that when these terms are used in this work, it is with the intent to be able to discuss a complex topic with defined terms.

In general, the distinction divides an overload-induced maladaptive process and an adaptation toward a gain in function. In disease the driving stimulus is mostly a decreasing

function. The inhibition of hypertrophy with β-adrenergic receptor blockers or RAAS inhibition had favorable outcomes, preventing LV dysfunction in both animal models and clinical trials [34]. Blocking or blunting cardiac hypertrophy has been an early therapeutic target in heart failure treatment [35] [36].

A long-standing hypothesis was corrected by Perrino and TAC-inventor Rockman. Their group was able to show, that the type of stimulus is the determining variable, not the duration. They developed an animal model with intermitted transverse aortic constriction (iTAC), where they were able to tighten and loosen the TAC ligation during each day. In this way they disproved the old hypothesis, that intermitting higher pressures could lead to favorable outcome. The iTAC mice went into failure, comparable to their "full-time" TAC cousins [37]. Intermittent pressure overload (iTAC) created a diastolic dysfunction, vascular rarefication and altered beta-adrenergic receptor function. A slight hypertrophy was established. The Perrino/Rockman group was able to reveal that the stress induced pathologic signaling was the driver of decreased cardiac function and not the duration of the stressor. Interestingly the iTAC model showed a diastolic dysfunction, decreased vascularization and altered b-adrenergic receptor function before the development of LV hypertrophy.
A hypertrophic response to pressure overload first decreases the wall stress per myofibril and creates mechanical advantages. Maintaining the ejection fraction in the presence of increased demand is the main goal of ventricular remodeling in athletes. What is really stunning and could be of great clinical importance, is the capability of a hypertrophied "athlete's heart" to go this path backward. Most investigators describe a full reversibility of hearts in de-training, leaving no pathological structural alterations behind [38] [39]. A study of 114 athletes, that took part in two to five consecutive Olympic Games, did not find increased adverse events or pathological remodeling [40].
But especially the very few athletes' hearts that are not fully reversible [41], offer a great chance to study what the differences are. Understanding the underlying mechanisms could offer clinicians the chance to direct a hyperopic response in a favorable way and utilize the adaptive potential of the body. Exercise offers a great potential to learn from the wisdom that resides within our bodies.

3.2.3. Energy metabolism and hypertrophy

In resting (normoxic) state, up to 95% of the hearts generated ATP comes from oxidative phosphorylation. The hearts mitochondria are therefore the most important source of energy production. Glycolysis and citric acid cycle only play a minor role during rest. 60-70% of the utilized ATP is needed for contractile function of the heart, the other 30-40% for various ion pumps [42] [43]. Energy substrates are ATP and phosphocreatine (PCr), with PCr being a buffer system for ATP transport. The heart itself only has a very limited high energy phosphate pool and is therefore dependent on fast ATP production. The main source (70-90%) for the substrates are fatty acids (FA). Further sources are glucose and lactate oxidation, and in minor percentages ketone bodies and amino acids. After meals, the fraction of glucose as a source of ATP production rises. With this background it is easy to imagine that disturbances in mitochondrial function and biogenesis have severe impact on energy supply of the heart. Impairments can lead to contractile dysfunction of the human heart [44]. Reduced substrate supply during metabolic stress seems to implement decreased mitochondrial capacity, leading towards reduced contractile force of the myocyte [45]. There is a tight regulation between the use of FA and glucose. The Randle cycle describes the phenomenon that the use of one of the substrates may directly inhibit the other. Regulators of the energy metabolism are for instance insulin and catecholamines, that have been reported to be at least partly involved in metabolic changes in the diseased heart.

In studies investigating advanced HFrEF in humans and rodents, ATP content, ATP flux and PCr/ATP content were reduced. These alterations were linked to diminished contractile function and accounted for the systolic dysfunction [46]. Therefore, changes in ATP handling could be a predictor in HF onset. Correspondingly, during adverse ventricular remodeling, mitochondrial reactive oxygen species (ROS) have been reported to be elevated [47]. Elevated levels of angiotensin II increased mitochondrial ROS, which lead to mitochondrial damage, MAPK upregulation and finally cardiac hypertrophy with fibrosis [48].

Adenosine monophosphate activated protein kinase (AMPK) is a sensor of energy stress and is activated through many pathways, including increases in ADP, ROS or Ca^{2+} load [49] [50]. Hypertrophy and HF are both associated with upregulated AMPK [51]. Further increase in AMPK in a HF model showed higher cardiac function with reduced remodeling of the LV. Plausible mechanisms are the generally upregulated energy supply, through both FA and glucose.

3.3. Opioids

Opioids have been utilized for centuries, especially in pain modulation. Even though they have been around for such a long time and have been used excessively and all over the world, the mechanisms of action are still poorly understood. The opioid research in the last decades was primarily focused on the central nervous system, trying to understand the pain modulating mechanisms and unravel its addictive properties.

New insights have been gained in context of exercise inducing endogenous opioid ligands and thus controlling adaptation. In recent years the cardioprotective properties of the opioidergic system have been of interest to numerous research groups.

3.3.1. Opioid receptors

So far four opioid receptor families have been discovered. Mu-, Kappa- and Delta- opioid receptors in the early 1990's, followed by the former orphan, opioid receptor-like orphan receptor (ORL), a few years later [52] [53]. They all belong to the large family of seven-transmembrane G protein-coupled receptors and they all show a high sequence homology. OR's are built of a single polypeptide chain and a seven-transmembrane-spanning helix, with the N-terminus extracellularly. The end is formed by a cytoplasmic C-terminal tail [54]. Recent findings created a concept of G protein-coupled receptor biased agonism, abandoning the old paradigm of binary, one receptor-one target mechanisms [55]. Here the different ligands lead to distinct receptor-effector complexes and stabilized receptor conformations. What follows are altered ligand binding and different levels of activation or inhibition of the subsequent signaling cascades. In a recent review, Campbell discussed the advantages and new possibilities of inhibiting specific G protein subunits instead of whole GPCR [56].

3.3.2. Opioid ligands

The endogenous ligands are not highly selective or specific to one opioid receptor [57]. There are several reasons that help to explain this:

1. MOR, KOR and DOR have many structural commonalities. They further have mutual function and cell-signaling mechanisms.

2. All endogenous ligands have a N-terminal residue Tyr, with the exception nociception, with a Phe. These residues are a requirement for interaction within the opioid receptor ligand binding domain.

3. They form homo-, heteromeric-complexes or even higher order oligomers, between opioid receptors and non-opioid receptors, altering their response to their ligands. These formations increase the spectrum of GPCR's regulatory mechanisms and may be essential for the fine-tuned regulations. An example of an "unlikely-couple"; Mu-opioid receptors and cannabinoid CB1-receptors can form a heterodimer and then signal through a common G protein [58 52 53 59 60 61].

The mammalian endogenous opioid peptides stem from three precursors, which translate from different genes [59]. They are named pro-opiomelanocortin (POMC). pro-enkephalin (PENK) and pro-dynorphin (PDYN). Heart cells store and release the endogenous opioid precursors [62]. Altered levels of endogenous opioid peptides were observed in pathological and physiological conditions, as well as under surgical interventions [63]. The endogenous opioid peptides bind with different affinities for the different opioid receptors, in both peripheral tissue as well as in the CNS. More than ten ligands have already been discovered, but the precursor for endomorphin remains unknown [64].

3.3.3. Opioids and exercise

In general, physical activity has beneficial effects on heart function and metabolism. Overall exercise stimuli can even be seen to be a necessary regulator to finetune the body. Even in cardiac disease, exercise has favorable effects on the heart and the whole organism. Nevertheless, diseased patients are not always capable to exercise to a level necessary to archive the benefits and initialize positive structural adaptations. Understanding the underlying mechanism could provide new therapeutic approaches to help these patients to benefit from exercise-like adaptations and thus become active again. Findings over the last years have linked exercise and endogenous opioid receptor ligands in the whole organism and the heart in particular.

Especially adaptation in performance and pain modulation have been associated. Pain modulation properties, with involvement of endogenous opioids, have been described during and after exercise regimes [65]. Further, involvement in positive changes of mood and anxiety have been studied and linked to endogenous opioids. Already in the late 90's, endogenous opioids were postulated to be involved in the positive immune system modulating effects of chronic exercise [66]. The type and duration of exercise seems to be

important for the profile of endogenous opioid peptides, the magnitude of plasma changes and the up or down regulating effects on the receptors. For example, upregulations in plasma beta-endorphin levels, were found in both male and female athletes, as well as in aerobic and anaerobic exercise [67]. In combination-trained female athletes also proenkephalin levels were significantly upregulated [68].

Animal models have been utilized to gain important insights on the mechanisms of endogenous opioids in exercise. Changes in neuronal μ, κ and σ opioid receptor binding and G protein activation have been described in rat after acute and chronic exercise regimes. The brain sections showed higher G protein activation, combined with lower opioid receptor binding, in response to 30-day exercise regime [69]. Peripheral delta opioid receptors reduced the exercise pressor reflex in femoral artery ligated rats. The investigators described a lesser pressor and cardio-accelerated response in animals that were treated with a DOR agonist [70]. Dickson *et al.* [71] postulated that the acute cardioprotective effects of exercise operate through an opioid dependent mechanism, that they blocked by naltrexone. The group described upregulated myocardial mRNA levels for opioid-system associated genes, and genes that control apoptosis and inflammation. In an IR-rat model, exercise induced cardio protection has been liked to DOR activation. The beneficial effects were significantly reduced with DOR specific pharmacological blockade, suggesting an important delta involvement [72]. In a similar study, a single dose of KORA (U50) right before IR, reduced infarct size. In the follow-up oxidative stress, development of fibrosis and increased neovascularization were achieved with KORA treatment. The same group demonstrated U50 induced protection against apoptosis in cultured myocytes, dependent on heme-oxygenase-1. They further detected increased Akt phosphorylation, that was PI3K dependent, and reduced IR induced apoptosis [73] [74].

3.3.4. Opioid receptors in cardiovascular disease

The analgetic use of Opioids is abundant in clinical every-day life for both acute and chronic pain management. Because of its relevance in analgesia the μ-opioid receptor has been in the focus of earlier research.
The following table gives a summary of studies testing the effects of MOR, DOR and KOR in CVD. Pharmacological testing revealed a number of receptor subtypes for all three OR [75], in investigative studies these subtypes are mostly not distinguished, based on very similar properties.

Table 2: Overview of selected studies on the topic of opioid receptors in CVD. By Deussen DN.

Receptor/ drug	Disease	Model	Key effect	Implicated targets/ effectors	Ref.
MOR					
MOR (DAMGO a MORA +/- beta- FNA; irreversible MOR antagonist)	Myocardial ischemia/ reperfusion injury	Rat heart *in situ*	IPC protection not dependent on MOR	Protection rather through DOR1	[76]
MOR (remifentanil)	Myocardial ischemia/ reperfusion injury	Rat heart *in situ*	Infarct size was reduced in preconditioning, postconditioning and continuous infusion	Remifentanil enhanced expression of anti-apoptotic protein Bcl2 and ERK1/2	[77]
MOR (fentanyl)l	Myocardial ischemia/ reperfusion injury	Rabbit heart *in situ*	Infarct size was reduced + antiarrhythmic effects	Involvement of peripheral and central ORAs	[78]
DOR					
DOR (selective agonist; naloxone)	Myocardial ischemia/ reperfusion injury	LAD occlusion (in dog)	Protection against ischemic injury and in mediation of ischemic preconditioning	Protection via the DOR-1	[79]
DOR antagonist naltrindole	Preconditioning →myocardial ischemia/reperfusion injury	LAD occlusion (in dog)	DOR antagonism abrogated the cardio protection induced by IPC	Drivers for DORA and ROS protection not found	[80]
Methadone & delta antagonist naltrindole	Myocardial ischemia	*In vitro* rat heart model	Block methadone's cardio protective effects with the DOR antagonist	DORA dependent protection	[81]
FIT (selective DORA)	Myocardial ischemia	*In vitro* rat heart model	Acute FIT administration reduced infarct size, when given before ischemia	Protection dependent on PI3K	[82]
KOR					
KORA (U50) +/-(nor-BNI, a selective κ-OR-antagonist)	Norepinephrine induced cardiac hypertrophy	*In vitro* neonatal rat cardiomyocytes	Inhibited cardiac hypertrophy, induced by norepinephrine	KOR dependent and by inhibiting sympathetic stimulation of the heart	[83]
KORA (U50) +/- (nor-BNI, a selective κ-OR-antagonist)	Isoprenaline induced cardiac hypertrophy	*In vivo* rat model	Inhibited cardiac hypertrophy, induced by β_1-adrenoreceptor stimulation	Antihypertrophic effects include calcineurin and ERK1/2	[84]
KORA (U50) +/- (nor-BNI, a selective κ-OR-antagonist)	Isoprenaline induced cardiac hypertrophy	*In vivo* rat model	Inhibited hypertrophy & showed reduced cardiac fibrosis	Reduced remodeling, maintained ECM	[85]

KORA (U50)	Isoprenaline induced cardiac hypertrophy	14-day rat model	Cardiac hypertrophy and fibrosis were reduced	Reduced oxidative stress + preserved expression of α-MHC	[86]
KORA (U50)	Myocardial ischemia/ reperfusion injury	LAD occlusion (in rat) & cultured rat cardio-myoctes	Reduced myocardial infarct size, oxidative stress, hypertrophy, and fibrosis, improved mechanical function, and greater neovascularization	Activation of HO-1 expression through the PI3K-Akt-Nrf2 pathway	[73]
KORA (U50) +/- (nor-BNI, a selective κ-OR-antagonist)	Myocardial ischemia/ reperfusion injury	LAD occlusion (in rat)	Antiarrhythmic effects	Activation of κ-OR accelerated recovery of pCx43 & total Cx43	[87]
KORA (U50) +/- (nor-BNI, a selective κ-OR-antagonist)	Myocardial ischemia/ reperfusion injury	LAD occlusion (in rat)	Reduced myocardial infarct sizes and myocardial apoptosis	KORA inhibits TLR4/ NF-κB signaling	[88]

3.4. RNA-sequencing

Fast progression has been made in the development of new methods for whole transcriptome characterization and quantification in recent years. Initial transcriptome analysis utilized hybridization-based microarrays. The so-called next generation sequencing, with RNA analysis via cDNA sequencing, allows high throughput database collection of the transcriptome. The advancement in data collection and pathway development has made it a groundbreaking tool in various areas of research [89]. Differential gene expression begins with RNA extraction, then it is followed by mRNA enrichment. The next step is cDNA synthesis and the preparation of an adaptor ligated sequencing library. With a high-throughput platform the library is then sequenced, with 10-30 million reads per sample. The gained readouts are then computationally processed, filtered and normalized between the samples. Further expression levels and significant changes run through statistical modelling.

Kyoto Encyclopedia at Genes and Genomes (KEGG) and Gene Ontology Consortium (GO) have been pioneering tools to perform organism specific enrichment analysis on data (gene, protein, small molecules) sets [90].

As genetic sequencing has shown that most eukaryotes share the core biological functions. GO consortiums goal is to unify the vocabulary and sort findings into three main categories, biological process, molecular function and cellular component, to form a common language [91]. The GO system of classification is a tool to hierarchically gene-products into a graph structure. With enrichment analysis the GO can be used to

functionally profile a set of genes and compare for example a group healthy to its pathological counterpart.

A major advantage of RNA-seq is the relatively unbiased approach, not always looking for the known, desired or obvious. In the controversially discussed field of opioids, carrying heavy luggage and prejudice, it is very important to be open minded. Hence, an unbiased look at the heart's whole transcriptome, holds high hopes in breaking new ground in heart failure research.

3.5. Transverse aortic constriction (TAC)

Transverse aortic constriction is a surgical technique developed by Howard D. Rockman at the University of California, San Diego [92]. TAC surgery is a highly validated model of pressure overload induced cardiac hypertrophy. The circumference of the aortic arch is decreased, leading to a "stenosis-like" pathology. The ligation is placed around the mid-aortic-arch between the brachiocephalic- and the left common carotid artery (Figure 6). To overcome this obstacle, the heart has to pump stronger to maintain a normal afterload. The TAC model is the gold standard for pressure overload induced left ventricular hypertrophy, on the path towards heart failure [93]. In contrast to chemically induced HF models, TAC does not have several toxic effects throughout the entire organism. And compared to complete occlusion of the left anterior descending (LAD) coronary artery [94], TAC shows a more gradual time course towards heart failure. LAD induces a MI like phenotype with a fibrotic scar tissue formation as well as a loss in contractile function.
TAC, performed by a skilled surgeon, is further advantageous with high success rates, low mortality and good reproducibility [95].

3.6. Opioid receptor agonism in pressure overload induced heart failure

3.6.1. Study outline

To investigate the above mentioned cardio protective properties of opioid receptor activation, our group conducted a novel study of ORA treatment in a murine TAC model. Preliminary data from the animal model was discussed in my *Master of Science (M.Sc.)* thesis [96]. In this work I described the phenotype of TAC induced LV-hypertrophy validated with echocardiography. Following is a short summary of our results at study end point ten weeks post TAC, eight weeks into treatment with either vehicle, KORA (U50) or DORA (FIT):

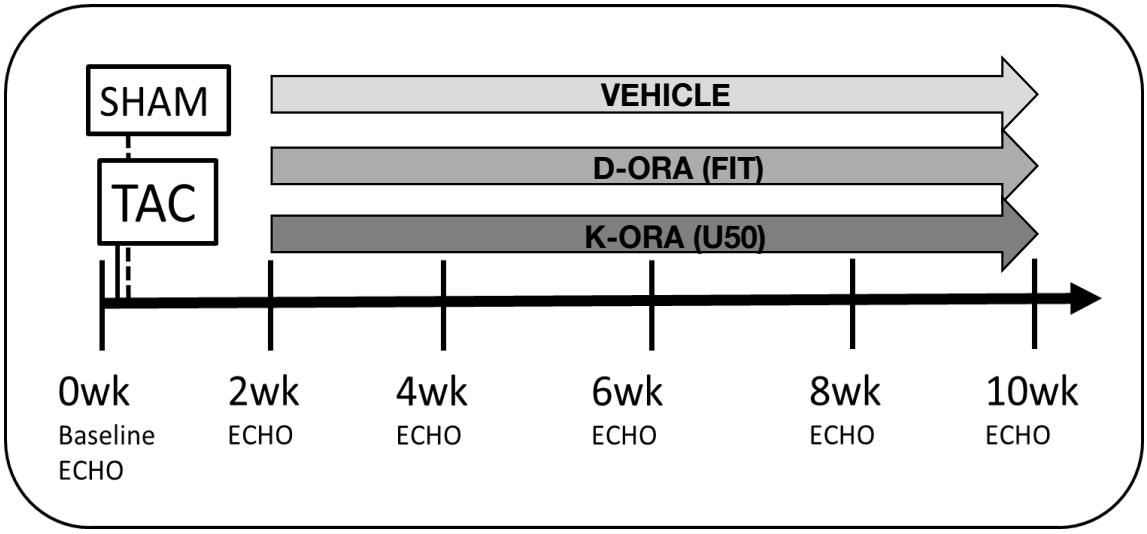

Figure 3: Study outline. Opioid receptor agonist (ORA) treatment after transverse aortic constriction (TAC) surgery. Fentanyl isothiocyanate (FIT), a selective and irreversible δ-opioid agonist and (±)-U-50488 hydrochloride (U50), a selective κ-opioid agonist. Body weight adapted ORA treatment followed from two-weeks post intervention. Echocardiography every two weeks from pre-TAC-surgery to study endpoint at ten-weeks. Graph by Deussen DN.

3.6.2. Pressure overload induced cardiac hypertrophy

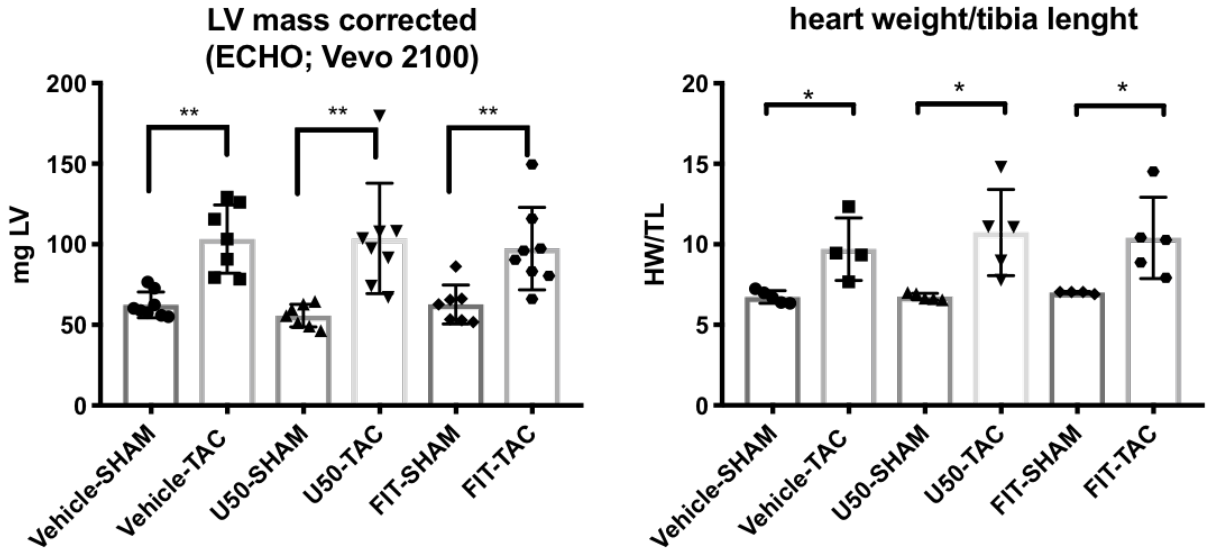

Figure 4: Left vetricular mass estimated by *in vivo* Echocardiography (Vevo 2100®); and *ex vivo* validation with calculated heart weight to tibia lenth; two tailed unpaired t-test, data presented as difference between means +/- SEM, adjusted p-values: * ≤ 0.05, ** ≤ 0.01, * ≤ 0.001, **** ≤ 0.0001.**

After ten weeks the hypertrophy in all three TAC groups was significant, in both *in vivo* Vevo®2100-calculated left ventricular (LV) mass and *ex vivo* heart weight/ tibia length (HW/TL). No difference in heart/LV mass could be detected between the three TAC groups. In SHAM animals the ORA treatment alone had no effect on LV size or heart weight.

3.6.3. Echocardiography

Measurements at study endpoint, after eight weeks of treatment, ten weeks post TAC/Sham surgery.

Table 3: Echocardiographic measurement at study end point 10wk post TAC, 8wk since treatment start. Veh = vehicle treated, U50 = kappa opioid receptor agonist U50, FIT = delta opioid receptor agonist FIT, Sham = mock operated, TAC = transverse aortic constriction operated group. Fraction shortening (%FS), ejection fraction (%EF), velocity of circumferential fiber shortening (Vcf). For statistical analysis between the groups 1-way ANOVA followed by a Tukey's multiple comparisons test was used. All values are presented as means ± standard deviation. Adjusted p-values are indicated as: * ≤ 0.05, ** ≤ 0.01, * ≤ 0.001, **** ≤ 0.0001. The groups consisted of an n of 6-7 animals.**

Group	%FS	%EF	Vcf
Veh-Sham	37.69 +/- 2.17	68.89 +/- 2.768	0.863 +/- 0.133
Veh-TAC	20.96 +/- 6.50	43.04 +/- 11.62	0.424 +/- 0.120
U50-Sham	41.57 +/- 3.90	73.56 +/- 4.25	0.980 +/- 0.083
U50-TAC	36.08 +/- 11.79	65.25 +/- 17.12	0.779 +/- 0.302
FIT-Sham	39.93 +/- 6.82	71.25 +/- 8.27	0.952 +/- 0.112
FIT-TAC	28.06 +/- 12.78	53.41 +/- 19.73	0.593 +/- 0.263

Veh-Sham vs Veh-TAC: *; U50-Sham vs U50-TAC: *; Veh-Sham vs Veh-TAC: *; U50-Sham vs U50-TAC: ns 0.053; Veh-Sham vs Veh-TAC: *; U50-Sham vs U50-TAC: ns 0.073; FIT-Sham vs FIT-TAC: *

At the study endpoint U50-TAC still showed no reduced FS compared to its Sham counterpart. In detail one animal showed a severe decrease in function, whereas the rest of the group still functioned comparable to U50-Sham. The difference in FS between Veh-TAC and U50-TAC remained significant from the 8wk to the 10wk timepoint (-15.12% +/- 4.985, $p \leq 0.0495$). Between these two groups the significant difference in Vcf got lost from the 8wk to 10wk timepoint ($p \leq 0.0736$). At the endpoint the FIT-TAC started to decline significantly in Vcf (-0.3597 +/- 0.1183; $p \leq 0.0486$), but with a very heterogeneous distribution within the group.

Table 4: Echocardiographic measurement at study end point 10wk post TAC, 8wk since treatment start. Left ventricular posterior wall dimensions in diastole (LVPWd), left ventricular posterior wall dimensions in systole (LVPWs). For statistical analysis between the groups 1-way ANOVA followed by a Tukey's multiple comparisons test was used. All values are presented as means ± standard deviation. Adjusted p-values are indicated as: * ≤ 0.05, ** ≤ 0.01, * ≤ 0.001, **** ≤ 0.0001. The groups consisted of an n of 6-7 animals.**

Group	LVPWs	LVPWd
Veh-Sham	1.086 +/- 0.034	0.714 +/- 0.039
Veh-TAC	1.184 +/- 0.122	0.953 +/- 0.107
U50-Sham	1.084 +/- 0.072	0.686 +/- 0.007
U50-TAC	1.417 +/- 0.101	1.024 +/- 0.063
FIT-Sham	1.183 +/- 0.066	0.749 +/- 0.075
FIT-TAC	1.251 +/- 0.077	0.952 +/- 0.065

The hypertrophy of the LVPW further increased towards the study endpoint. All TAC groups showed a similar thickness of the LVPW during diastole. However, during systole the U50-TAC hearts were significantly thicker than both Veh-TAC (-0.2348mm +/- 0.05048; $p \leq 0.0007$) and FIT-TAC (-0.1681mm +/- 0.0548; $p \leq 0.0244$). We saw a loss of contractile function in the left ventricle only in the Veh-TAC and FIT-TAC groups, whereas the U50-TAC showed a solid hypertrophic response with maintained LV contractility.

3.6.4. Key findings of ORA treatment in our TAC model

- In pressure overload challenged mice heart function was preserved with KORA treatment when compared to vehicle treatment.

- The positive effect of KORA treatment was significant, the DORA treatment showed no significant advantage over vehicle treatment.

- Myocardial hypertrophy was not reduced in both ORA treated TAC groups, but only KORA treatment showed preserved contractility.

4. Hypothesis

The cardioprotective potential of κ/σ opioid receptors should be further explored in the TAC mouse model of pressure overload, as they might hold valuable therapeutic potential. Our specific questions are:

1. Are structural advantages of ORA treated animals evident in histological analysis?

2. Is RNA-sequencing a valid tool to detect the relevant differences between the groups in disease progression?

3. Hypertrophy was not reduced in ORA treated TAC groups, but KORA treatment showed preserved contractility. What are the mechanisms behind this favorable outcome?

5. Methods

5.1. Animal model

Animals

Male C57Bl/6J mice were purchased from Jackson Laboratories (Bar Harbor, ME).
The U.S. Academy of Science Guide for the Care and Use of Laboratory Animals was the basis for all animal experiments. Animal protocols were approved by the VA San Diego Healthcare System Institutional Animal Care and Use Committee. Housing was provided in a temperature-controlled facility with *ad libitum* access to food and water and kept on a 12-hour light and dark cycle.

Transverse Aortic Constriction – Surgery

The TAC surgery was performed on eight to ten-week-old animals, as established and described by H. Rockman at UCSD [92]. Briefly, the mice were prepared for surgery, hair was removed from the chest and neck area. Anesthesia induction was obtained through a nosecone, with 1-1.5% Isoflurane. A 274-heating pad (Cincinnati Sub Zero, Cincinnati, OH) was placed under the surgical field to prevent hypothermia. A sterile field was created, the animal was covered, sparing the neck and chest area. Repetitive application of bromide and 70% ethanol were used to disinfect the surgical area. During surgery animals were intubated and mechanically ventilated. A correct intubation was ensured by an incision at the ventral side of the neck which exposed the trachea. The aortic arch was prepared through an incision at the second intercostal space. A 7-0 silk suture was placed between the brachiocephalic artery and the left common artery. To standardize the degree of ligation a 27G needle was positioned between the aortic arch and the suture. The suture was then tied against the needle with two double surgical knots, before removing the needle. Sham animals handled equally in all aspects of the surgery, besides here the suture was only placed and not tied. Success of the surgery, a significant hypertrophic response of the left ventricle, was evaluated with echocardiography.

Pain relieve after surgery is usually gained with barbiturates or opioids in this setting. To exclude an interfering effect in our experimental design, we had to exclude these pain-relieving drugs.

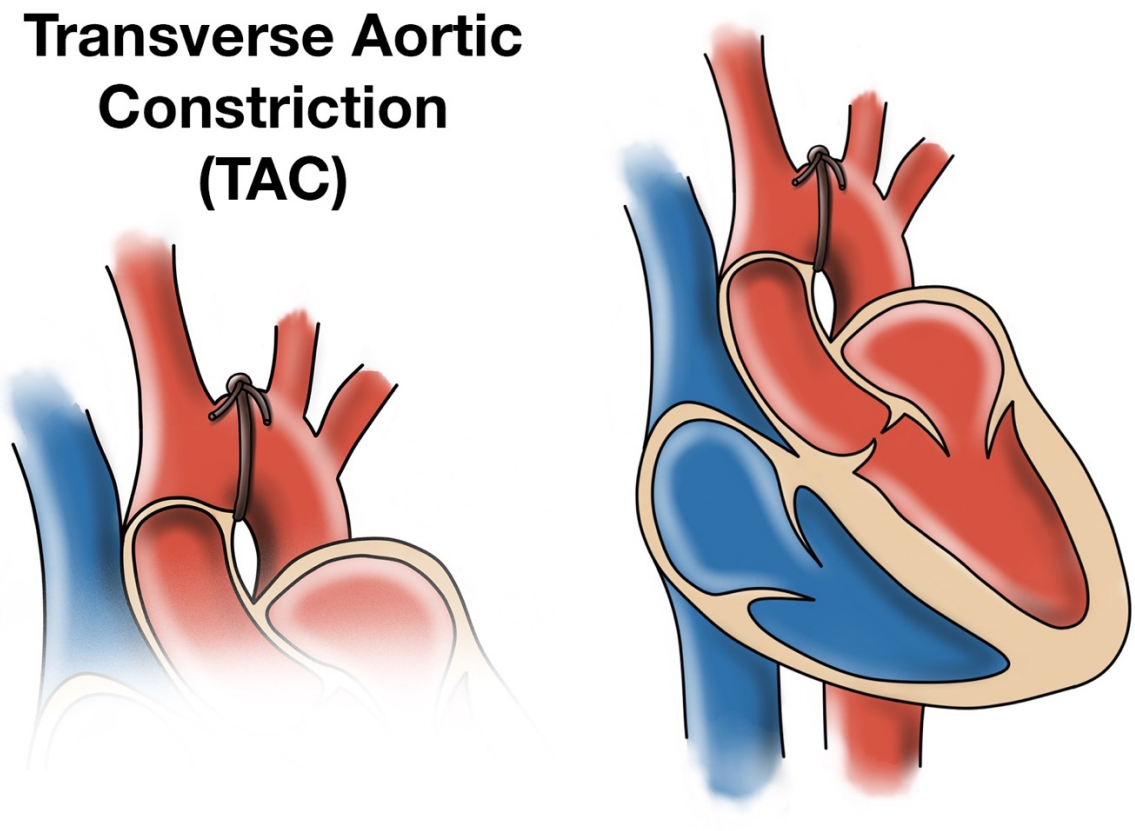

Figure 5: Aortic arch with transverse aortic constriction (TAC). The suture is placed between the brachiocephalic artery and the left common artery. By Huebner T & Deussen DN.

5.2. Opioid receptor agonist treatment

Fentanyl isothiocyanate (FIT)

FIT is a selective and irreversible δ-opioid agonist.
The treatment dose for the delta agonist and the interval of injections were based on preliminary results and an ex vivo study by a collaborative group, that investigated the cardioprotective properties of FIT [82]. 10µg/kg were administered *i.p.* every 72 hours.

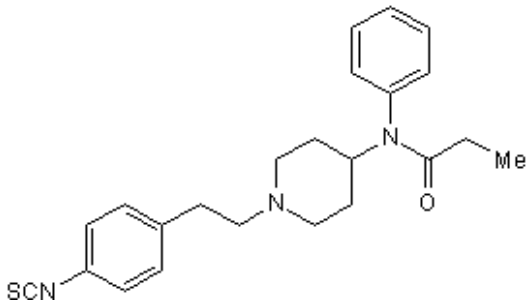

Figure 6: Molecular structure FIT;
data sheet from TOCRIS, https://www.tocris.com/products/fit_1480

Chemical Name: N-[1-[2-(4-Isothiocyanatophenyl)ethyl]-4-piperidinyl]-N-phenylpropanamide
Formula: C23H27N3OS
Molecular weight: 393.55
Purity: >99.4%
Catalog #1480, (TOCRIS Bioscience, Bristol, UK)

(±)-U-50488 hydrochloride (U50)

U50 is a selective κ-opioid agonist
1.25mg/kg U50 were injected *i.p.* every 24 hours, based on previous findings showing reduced hypertrophic response and fibrosis formation *in vivo* [85].

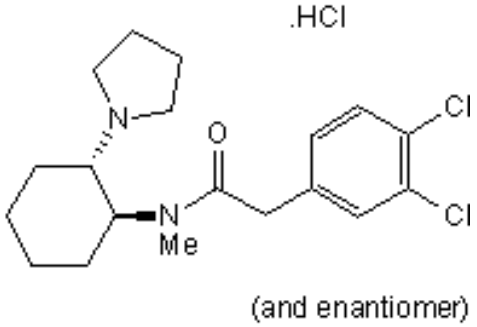

Figure 7: Molecular structure U50;
data sheet from TOCRIS, https://www.tocris.com/products/plus-u-50488-hydrochloride_0471

Chemical Name: trans-(±)-3,4-Dichloro-N-methyl-N-[2¬-(1-pyrrolidinyl)cyclohexyl] benzeneacetamide hydrochloride
Formula: C19H26Cl2N2O.HCl

Molecular weight: 405.79
Purity: >99.6%
Catalog #0495, (TOCRIS Bioscience, Bristol, UK)

5.3. Study endpoint measurements and tissue preparation

The bodyweights of the animals were documented at study endpoint. Euthanization was attained with a lethal pentobarbital dose of 160mg/kg. The intra-peritoneal injection was equally distributed in both flanks. The chest cavity was then opened, the heart exposed and removed. Excess blood was removed before the heart before weights were determined. To prepare the heart tissue for following analysis, all hearts were handled in the same manner, as described in Figure 8. With a razorblade, a cut was executed to separate the two atria together with the superior part of the ventricles from lower 2/3 of the RV and LV. The segment Nr.1 was further dried off and embedded in Tissue Tek (Sakura, Torrance, CA), frozen in a bath of dried ice and 2-Methylbutane (J.T.Baker®, Pleasant Prairie, WI) and stored at -80ºC. The segment (1) of the superior right ventricle and left ventricle was prepared for further immunohistochemical analysis. As sample for RNA sequencing the segment Nr.2, with a weight of 20-25mg, was dissected from the left ventricle before shock-freezing in liquid nitrogen. The same freezing procedure was followed for segment Nr.3, consisting of right ventricle, septum and left ventricle. Lung tissue und skeletal muscle (m. gastrocnemius and m. tibialis anterior) were frozen and conserved at -80 ºC, for further analysis.

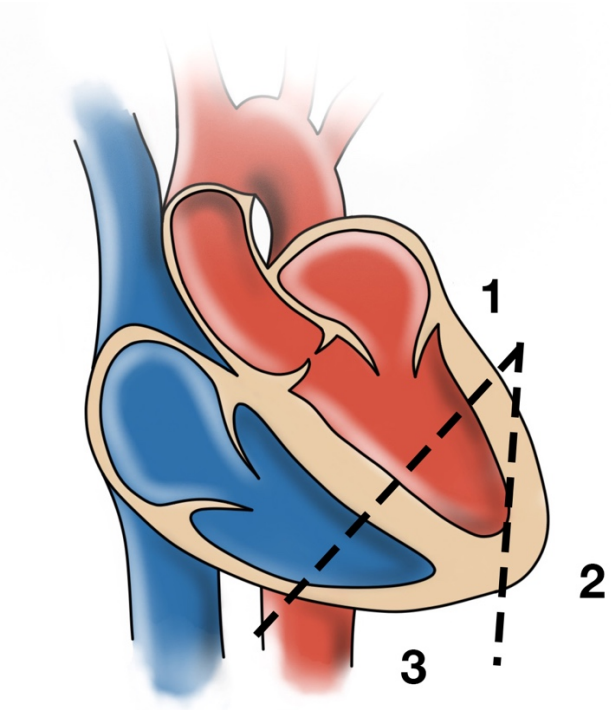

Figure 8: Heart sections. 1 Heart base with both atria and upper half of the left and right ventricle, 2 Left ventricle, 3 Left ventricle, right ventricle and septum. By Huebner T & Deussen DN.

5.3.1. Light microscopy

For hematoxylin and eosin (HE) or picrosirius red staining frozen heart samples were cut into 3-4µm thick slices with a HM525 NX Cryostat (Thermo Scientific, Waltham, USA).
The slides were then fixated with zin-formalin (Anatech, Battle Creek, USA) and later washed in deionized water. For HE cell nuclei were subsequently stained with Harris hematoxylin (Sigma-Aldrich, Saint Louis, USA) and differentiated with 70% ethanol, containing 120mM hydrochloric acid. The slides were then counterstained in alcoholic eosin with Phloxine B™ (Sigma-Aldrich, Saint Louis, USA). For picrosirius red, after postfixing the slides in saturated picric acid aqueous solution, slides were stained for one hour in .1% sirius red F3B (Sigma-Aldrich, Saint Louis, USA) in saturated aqueous picric acid solution. For both staining's a dehydration followed before the slides were cover-slipped with Permount Mounting Medium™ (both Thermo Scientific, Waltham, USA) and then dried for 48h.
Images were viewed and pictures were taken with a BZ-X710 all-in-one microscope (Keyance, El Segundo, USA).

5.3.2. Transmission electron microscopy

For Transmission electron microscopy (TEM), two animals per group were selected on the basis of the average values of contractile heart function (%FS). Hearts were prepared for TEM as follows:

1. Hearts were transcardially-perfusion-fixed with 2% paraformaldehyde and 2.5% of glutaraldehyde in 0.15M sodium cacodylate buffer (buffer pH 7.4).
2. 1% osmium in 0.15M sodium cacodylate for 1-2 hours on ice.
3. 5x10 minutes washed in 0.15M sodium cacodylate buffer followed by rinsing in ddH_2O on ice.
4. Incubated in 2% of UA for 1-2 hours at 4 °C.
5. Dehydration in ETOH: 50 %, 70 %, 90%, 2x100%. Each time 10 minutes on ice.
6. Next, samples were moved into dry acetone for 15 minutes at RT.
7. 50:50 ETOH: Durcupan™ (Sigma-Aldrich, Saint Louis, USA) for 1 hour at RT.
8. 100% Durcupan™ overnight.

On the following day, tissues were put into fresh 100% Durcupan™ for 1/2 day at RT.
In Durcupan™ embeded tissues were put in oven at 60 °C for 36 to 48hrs.
Ultrathin sections of 60nm were cut on a Leica (Wetzlar, Germany) microtome with a diamond knife and stained with uranyl acetate and lead. Images were viewed with the FEI Tecnai Spirit G2 BioTWIN Transmission Electron Microscope (at 80 kV) and captured with a bottom mount Eagle 4k (16 megapixel) camera (Hillsboro, USA).
The protocol was developed by Ying Jones and the EM core at UCSD.

5.3.3. Weight ratios

To determine weight ratios heart weight (HW), body weight (BW) and tibia length (TL) were measured. HW to BW is commonly used to confirm cardiac hypertrophy, normalized to the animal's body weight. To verify BW-independent increases in HW the HW to TL ratio was employed.

5.4. Echocardiography

Echocardiography procedures and calculations were described in detail in my M.Sc. Thesis [96]. Following is a brief overview for better understanding:

The Vevo®2100 (Visulasonics, Toronto, Canada) was used for echocardiography (ECHO), the data was analyzed with the Vevo®LAZR System software v1.4.1.
For all mice, the first ECHO was completed before TAC (PRE) and followed with consecutive measurements in a two-week interval, as described in study outline (Figure 3). At a heart rate of 550-620 bpm the systolic function was measured. Anesthesia was obtained with 0.7-1.2% isoflurane and 1 L/min oxygen, via nosecone.
The number (n) of animals per group was 6-8 for echocardiographic measurements. Measurements were obtained in B-Mode and M-Mode. Fraction shortening (FS), ejection fraction and LV mean velocity of circumferential fiber shortening (Vcf) were calculated as measurements of myocardial function. Further, wall dimensions in systole and diastole were measured [97].

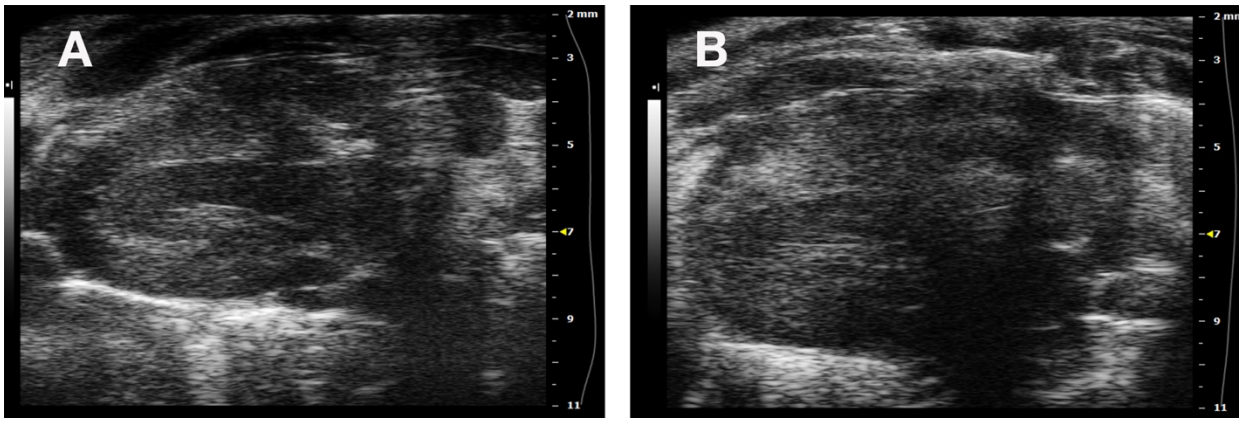

Figure 9: B-Mode of mouse #621. Pre-TAC (A) and 10-weeks post-TAC (B). Verification of LV hypertrophic response to TAC surgery.

Table 5: Formulas of functional echocardiographic measurements. Left ventricular internal dimensions in diastole (LVIDd), left ventricular internal dimensions in systole (LVIDs), aortic ejection time (AET)

Functional measurement	Formula
Fractional shortening	$\%\mathrm{FS} = \left[\frac{\mathrm{LVIDd} - \mathrm{LVIDs}}{\mathrm{LVIDd}}\right] \times 100$
Ejection fraction	$\%\mathrm{EF} = \left[\frac{\mathrm{LVIDd}^3 - \mathrm{LVIDs}^3}{\mathrm{LVIDd}^3}\right] \times 100$
The LV mean velocity of circumferential fiber shortening	$\mathrm{Vcf} = \frac{\mathrm{LVIDd} - \mathrm{LVIDs}}{\mathrm{AET} \times \mathrm{LVIDd}}$

5.5. Expression analysis

RNA extraction

RNA was extracted from frozen, 15-20mg LV samples, utilizing the Qiagen (Valencia, CA) RNeasy® Fibrous Tissue Mini Kit. The companies' standard protocol was followed:

- Add 10µl β-mercaptoethanol (β-ME), or 20µl 2M dithiothreitol (DTT), per 1ml Buffer RLT before use.
- Add 4 volumes of ethanol (96–100%) to Buffer RPE for a working solution.
- Prepare DNase I stock solution. Dissolve the lyophilized DNase I in 550µl RNase-free water by injecting the RNase-free water into the vial using an RNase-free needle and syringe. Mix gently by inverting the vial. Do not vortex. Store DNase I as single-use aliquots at –20°C for up to 9 months or at 2–8°C for up to 6 weeks.

1. Heat water bath or heating block to 55°C.
2. Disrupt and homogenize ≤ 30mg tissue in 300µl Buffer RLT using the TissueRuptor®, TissueLyser LT or TissueLyser II.
3. Add 590µl RNase-free water, then 10µl proteinase K, mix and incubate at 55°C for 10 min.
4. Centrifuge at 10,000 x *g* for 3min.
5. Transfer supernatant to new tube. Add 0.5 volumes of 96–100% ethanol, and mix. Do not centrifuge.
6. Transfer 700µl of sample to RNeasy Mini column (in a 2ml collection tube). Close lid, centrifuge for 15 s at ≥ 8000 x *g* and discard flow-through. Repeat step until complete lysate is used.
7. Add 350µl Buffer RW1 to RNeasy column. Close lid, centrifuge for 15s at ≥ 8000 x *g* and discard flow-through.

8. Mix 10µl DNase stock solution with 70µl Buffer RDD, add to RNeasy membrane and incubate for 15min at 20–30°C.
9. Add 350µl Buffer RW1 to RNeasy column. Close lid, centrifuge for 15s at ≥ 8000 x *g* and discard flow-through.
10. Add 500µl Buffer RPE to RNeasy column. Close lid, centrifuge for 15s at ≥ 8000x *g* and discard flow-through.
11. Add 500µl Buffer RPE to RNeasy column. Close lid, centrifuge for 2min at ≥ 8000x *g*.
12. Place RNeasy column in new 1.5ml tube. Add 30–50µl RNase-free water, close lid and centrifuge for 1min at ≥ 8000 x *g*.

Source: **www.qiagen.com/HB-0485** (*RNeasy Fibrous Tissue Handbook*)

RNA quantification

NanoDrop™ 3300 (Thermo Scientific, Walham, MA) was utilized to measure RNA purity levels. Pure RNA has an A260/A280 ratio of ~ 2.1. Values of 1.8 – 2.1 were considered to be of acceptable purity. Lower values indicate protein or DNA contamination. The threshold for A260/A230 ratio was > 2.0, as lower values are regarded as contamination with wash-solution or others. 1µl of RNA extract was used for NanoDrop™ RNA quantification. After quantification all samples were diluted equally in RNase free water and frozen at -80°C for further analysis.

RNA quality control

RNA integrity was checked by Agilent Bioanalyzer 2100 (Santa Clara, CA); only samples with clean rRNA peaks were used for further experiments.

RNA sequencing

RNA sequencing was performed by QuickBiology (Pasadena, CA), according to their standard protocol. Six to eight animals were analyzed per treatment group. The library for RNA-Seq was prepared according to KAPA Stranded mRNA-Seq poly(A) selected kit with 300bp insert size (Wilmington, MA) using 250ng total RNAs as input. Final library quality and quantity was analyzed by Agilent Bioanalyzer 2100 and Life Technologies Qubit 3.0 Fluorometer. 150bp paired end reads were sequenced on Illumina HighSeq 4000 (San Diego, CA).

5.6. Statistical analysis

GraphPad Prism® (La Jolla, CA) version 8.0 was used for statistical analysis of heart weight ratios and echocardiographic measurements. All values are presented as means ± standard deviation (±SD). For parametric data the statistical analysis was performed with unpaired Student's t-test (2-tailed testing). For statistical analysis in experiments with more than two groups we used an analysis of variance (1-way ANOVA) followed by a Tukey's multiple comparisons test, when indicated.

Adjusted p-values are indicated as: * ≤ 0.05, ** ≤ 0.01, *** ≤ 0.001, **** ≤ 0.0001.

RNA Sequencing statistical analysis

The sequencing reads were first mapped to the latest UC Santa Cruz transcript set using Bowtie2 version 2.1.0 [98] and the gene expression level was estimated using the RSEM software (v1.2.15) [99]. Trimmed mean of M-values (TMM) was used to normalize the gene expression. Differentially expressed genes were identified using the edgeR program [100]. Genes presenting altered expression with $p < 0.05$ and more than 1.5-fold changes were considered differentially expressed. Goseq [101] was utilized to perform the Gene Ontology (GO) enrichment analysis and Kobas [102] was used to make the pathway analysis. GO provides a system of classifying genes to their assigned functional characteristics [103]. GO is used to cluster sets of genes and gene products depending on their function and compare between treatment groups [90].

The volcano plot is a type of scatterplot that displays the extent of change (fold change) versus the statistical significance (p-value). In this way it enables a quick way to identify genes with large fold change and statistical significance [104]. The volcano plot is composed by plotting the negative log of the p value on the y axis (base 10), data points with low p-values appear toward the top of the plot. The x-axis of the plot is the log of the fold change between the two conditions.

Heatmaps show gene expression of the high-throughput data using two dimensional tables as shades of colors [105]. Green shows down-regulation in gene activity, red up-regulations accordingly, color shades indicate the fold-change. Every row on the X-axis represents a single animal.

6. Results

6.1. Microscopy

6.1.1. Light microscopy - picrosirius red staining

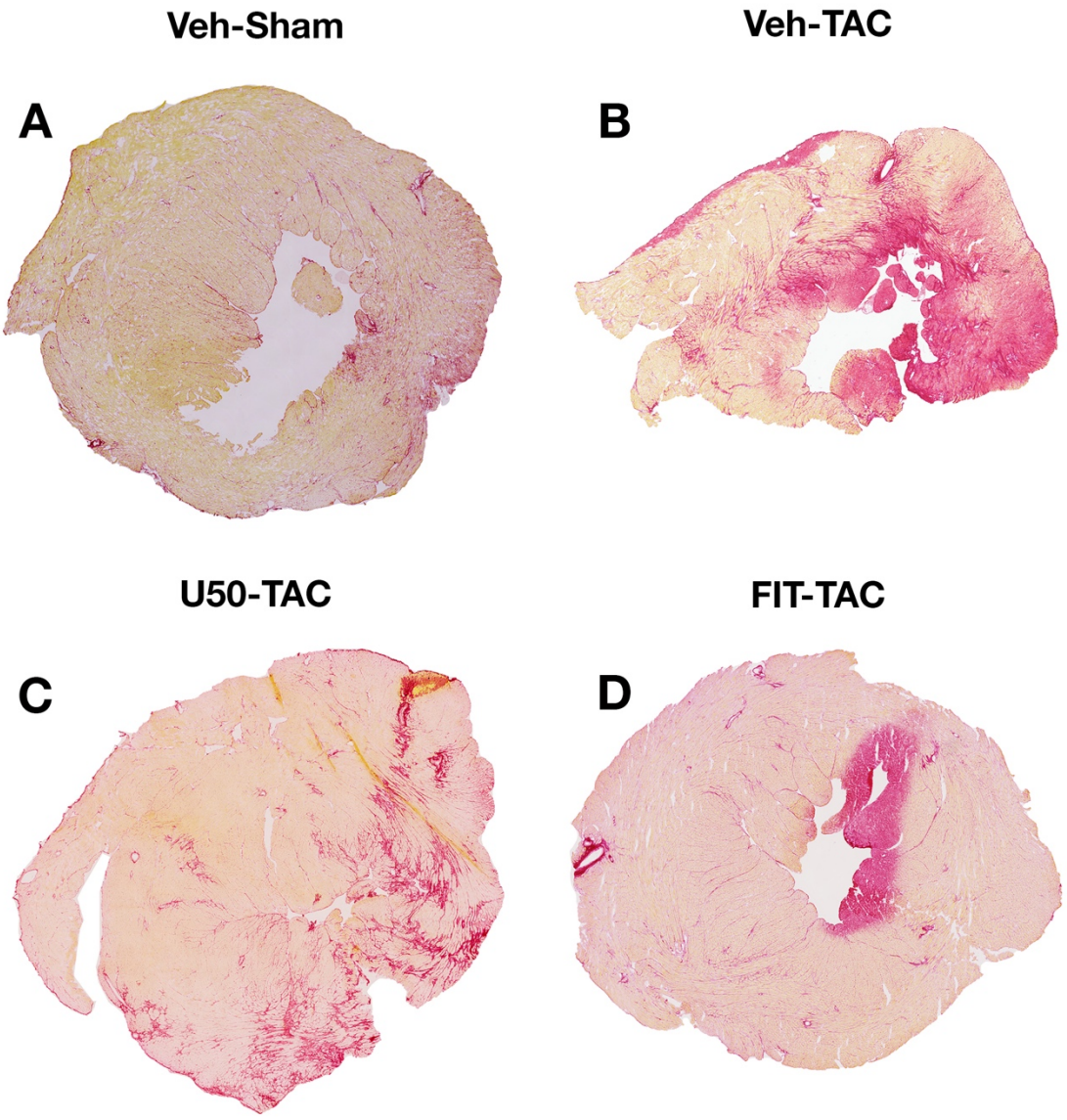

Figure 10: Overview of the left ventricle in picrosirius red staining, showing cardiac fibrosis and hypertrophy. Dark red staining indicates areas of high collagen composition. A. Veh-Sham, B. Veh-TAC, C. U50-TAC and D. FIT-TAC; Figure by Kopp EL and Deussen DN.

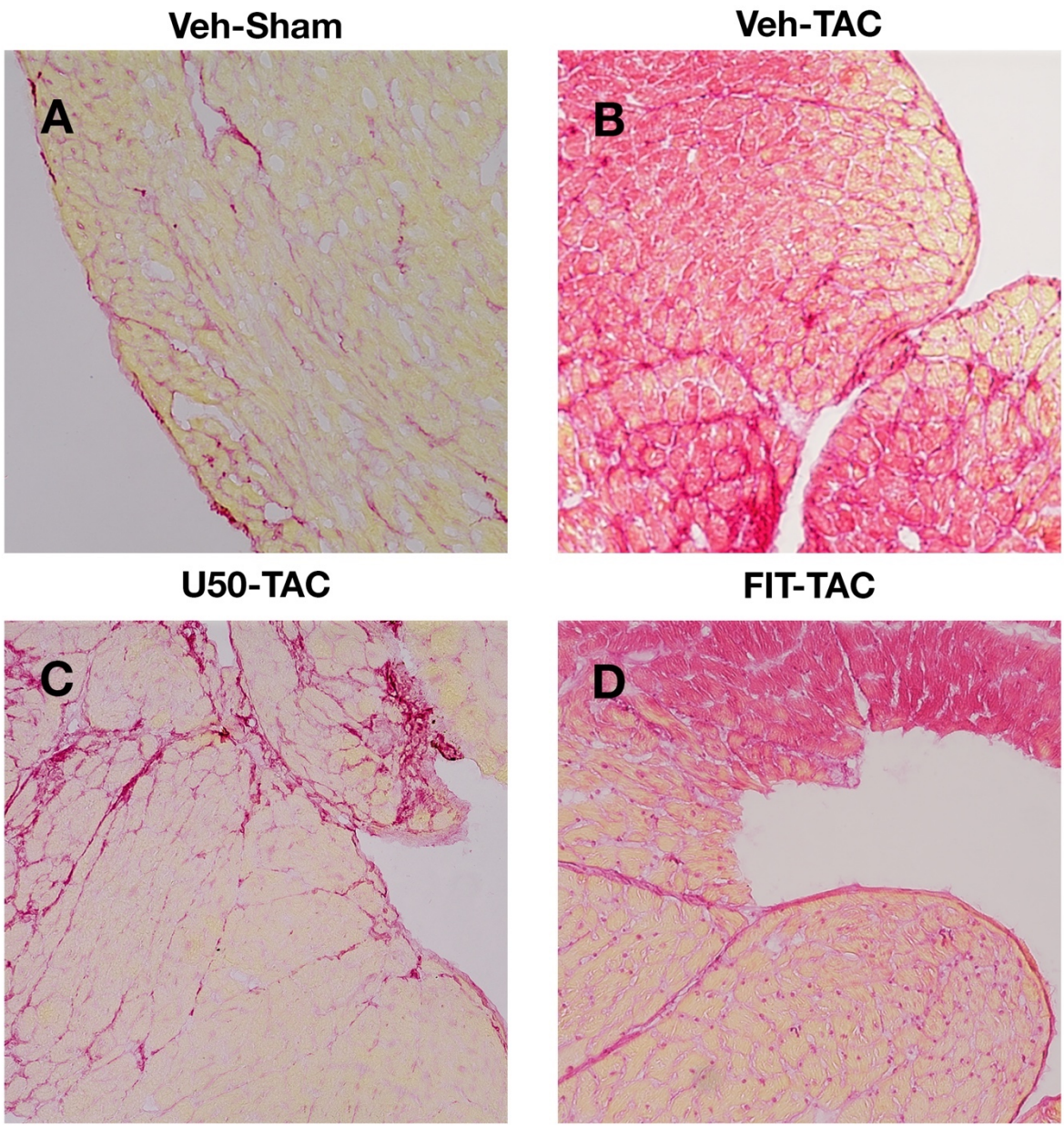

Figure 11: Detailed view of collagen distribution through picrosirius red staining. Dark red staining indicates areas of high collagen composition. A. Veh-Sham, B. Veh-TAC, C. U50-TAC and D. FIT-TAC; Figure by Kopp EL and Deussen DN.

Left ventricles of TAC mice stained with picrosirius red show increased collagen proportions compared to sham hearts. Myocardial collagen content in vehicle TAC was higher than in ORA treated animals.

6.1.2. Light microscopy - hematoxylin and eosin

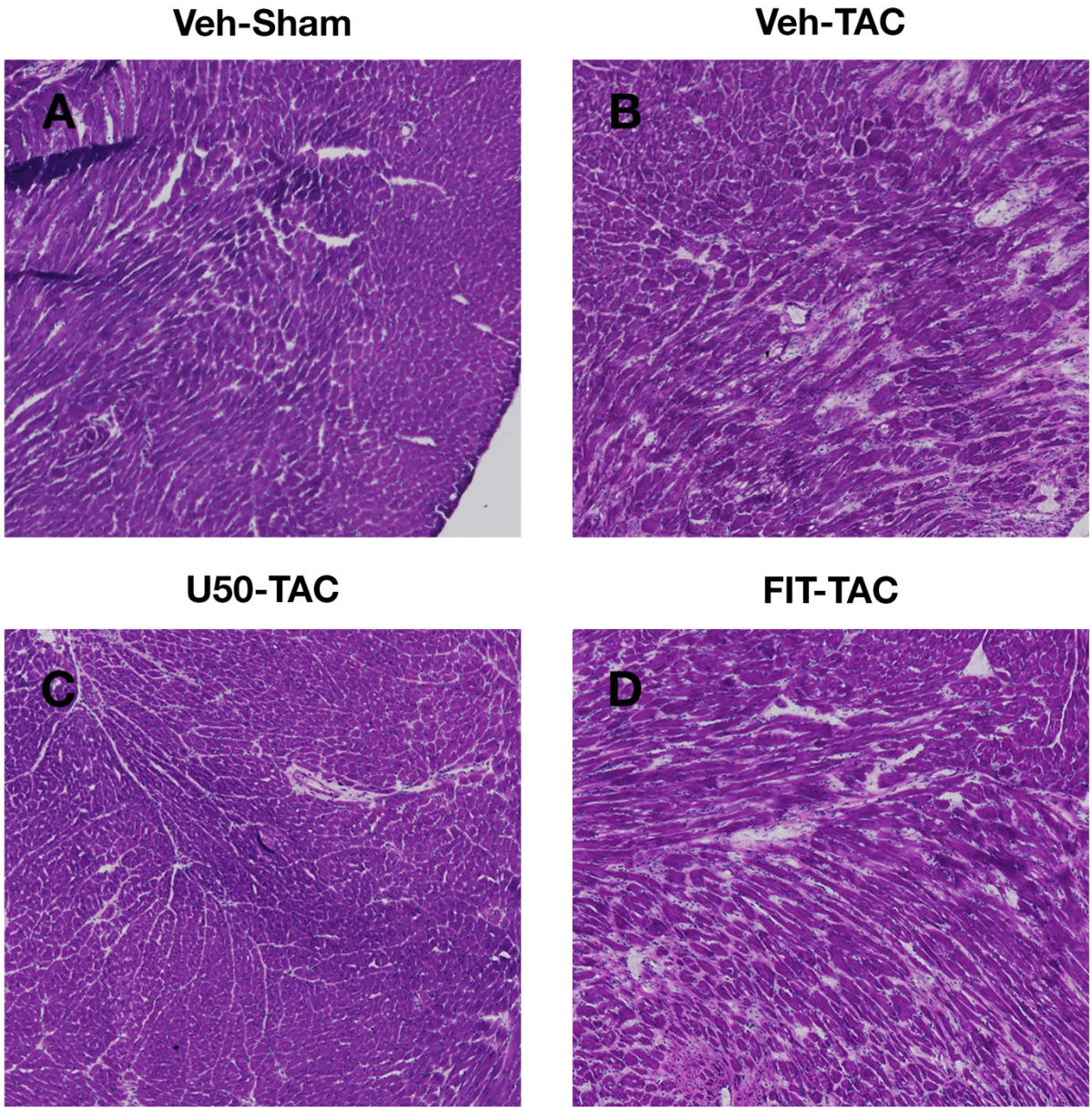

Figure 12: Hematoxylin and eosin (HE) staining (4x) pictures comparing the structural integrity of the heart. A. Veh-Sham, B. Veh-TAC, C. U50-TAC and D. FIT-TAC; Figure by Kopp EL and Deussen DN.

The HE microscopic images showed a heart structure in U50-TAC that is closer to the sham animals, than that of Veh-TAC or FIT-TAC. In comparison to the other two TAC groups U50-TAC seemed to have less disrupted myocyte alignment and slighter fibrosis. On first sight, it appeared that the hypertrophic response in U50 was more physiological. These findings in the microscopic images were consistent with the maintained contractile function (Table 3).

DORA treatment (FIT-TAC) did not seem to have these positive structural benefits (D). Therefore, for a better visualization, the following TEM chapter concentrates on U50 vs vehicle comparison.

6.1.3. Transmission electron microscopy

Overview images of sarcomere structure

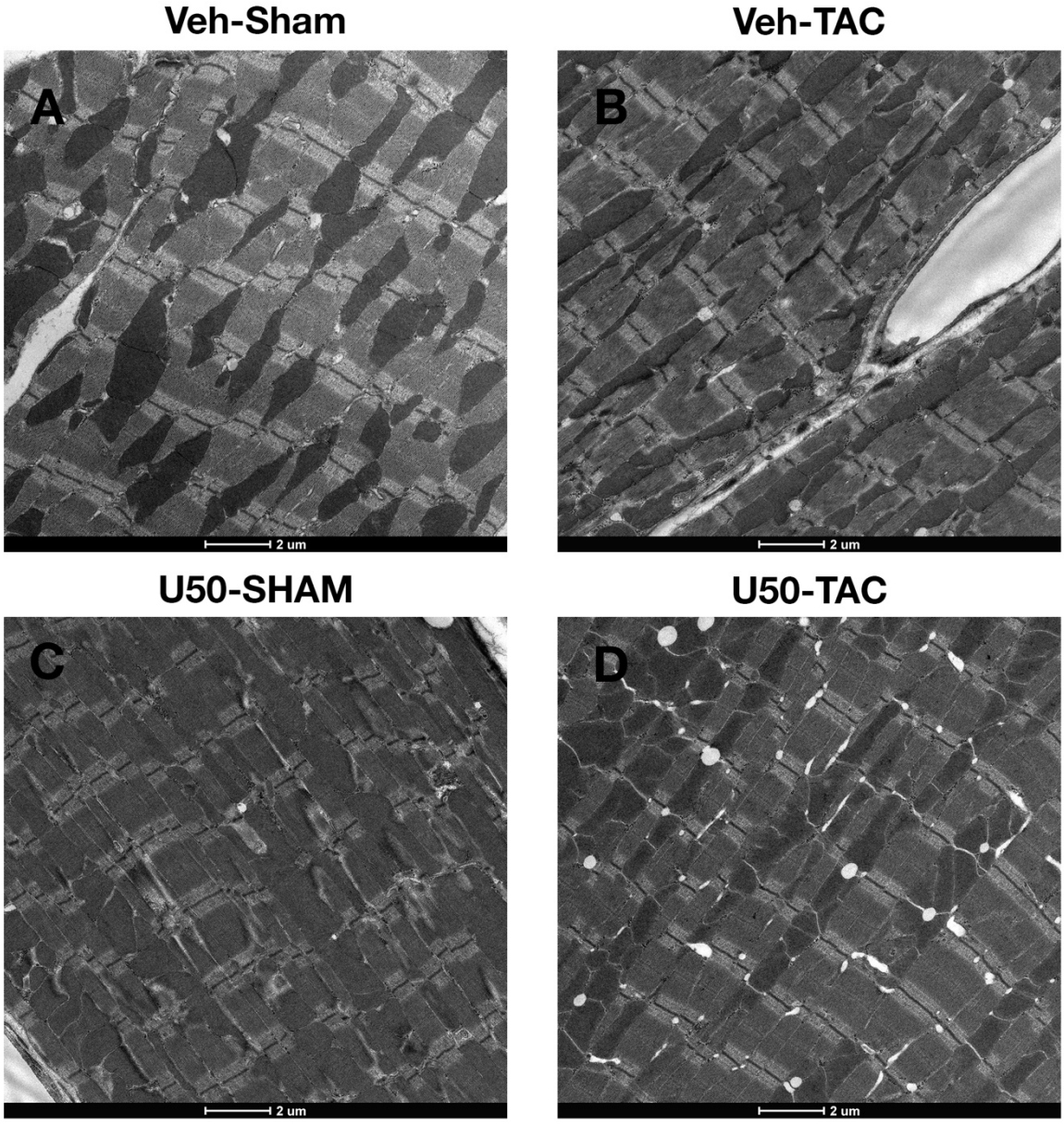

Figure 13: TEM images 2900x, Sarcomeres of U50 vs vehicle treatment. A. Veh-Sham, B. Veh-TAC, C. U50-Sham and D. U50-TAC; Figure by Kopp EL, Zemljic-Harpf AE and Deussen DN.

Transmission electron microscopy of heart samples comparing the structural integrity of the left ventricle showed in U50-TAC a more physiological hypertrophy with intact ultrastructure, compared to Veh-TAC.

Heart ultrastructure with mitochondria

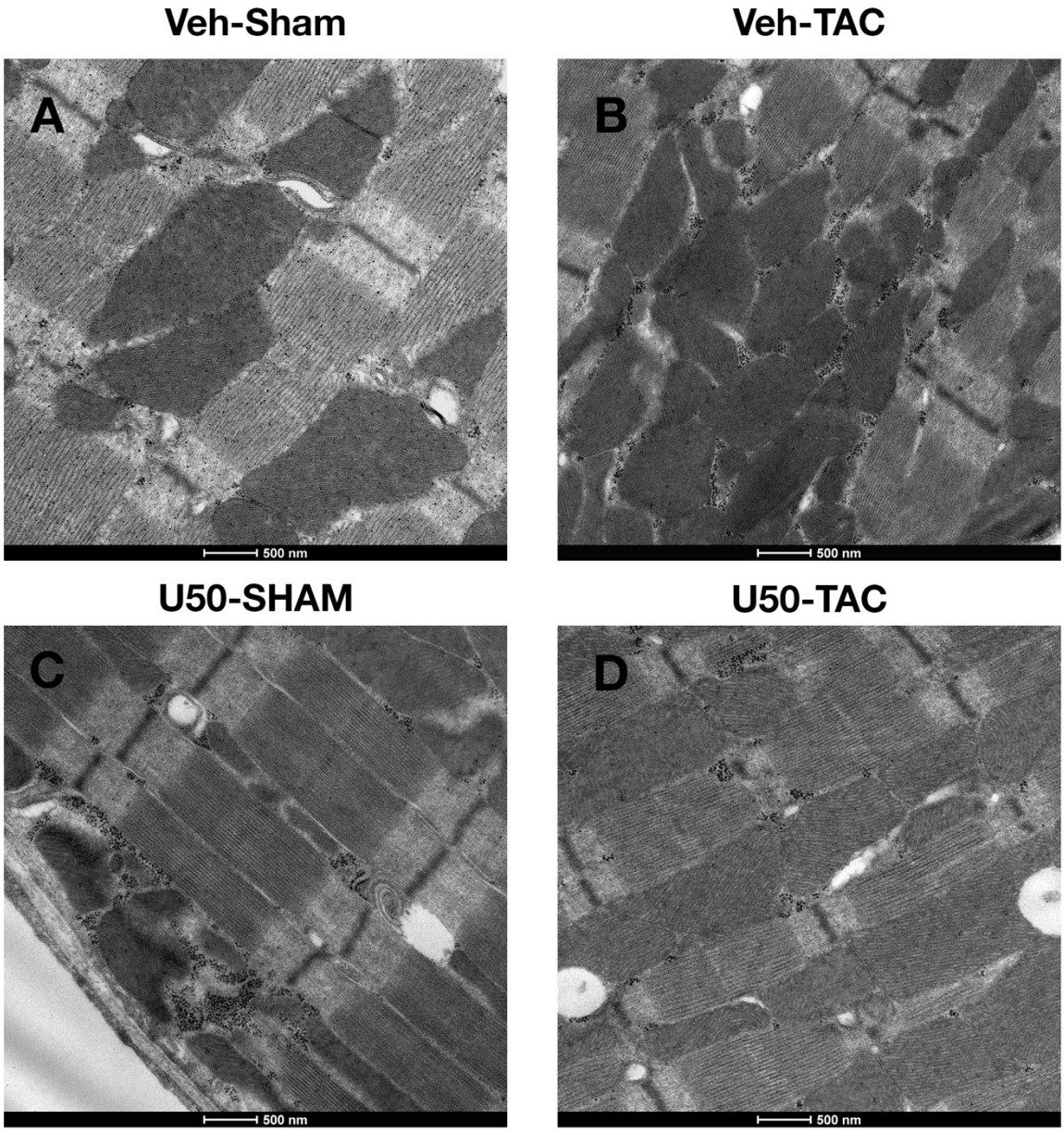

Figure 14: TEM images 9300x, mitochondria of U50 vs vehicle treatment. A. Veh-Sham, B. Veh-TAC, C. U50-Sham and D. U50-TAC; Figure by Kopp EL, Zemljic-Harpf AE and Deussen DN.

On further magnification at 9300x we compared mitochondrial integrity in the left ventricle of our treatment groups. Mitochondria of U50-TAC looked more aligned and integrated into the muscular structures compared to vehicle TAC.

Endothelium and caveolae

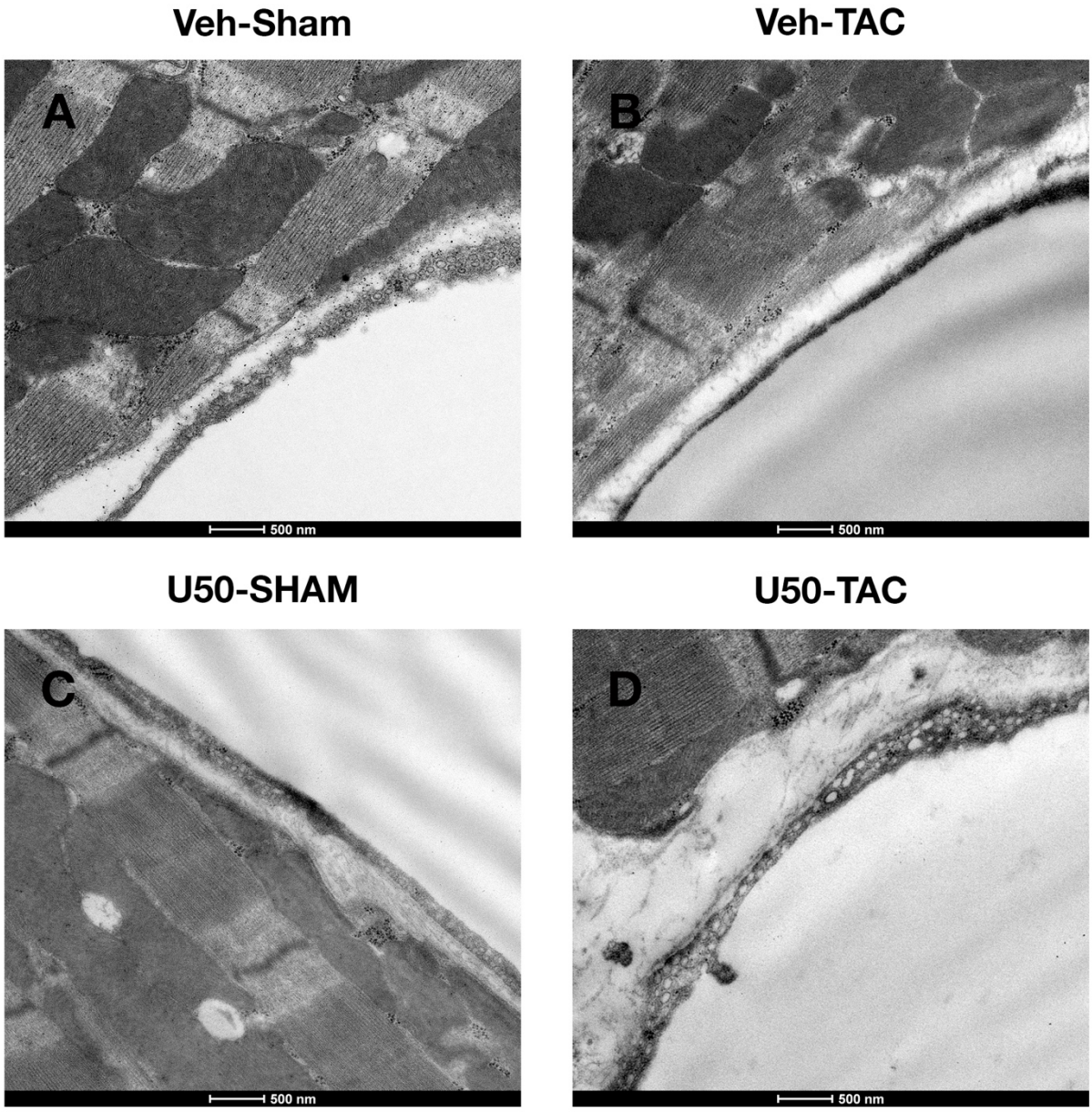

Figure 15: 9300x TEM images of A. Veh-Sham, B. Veh-TAC, C. U50-Sham and D. U50-TAC. U50-TAC showed preserved endothelial cell (EC) caveolae when compared to Sham, while Veh-TAC had a caveolae depletion in the EC. Figure by Kopp EL, Zemljic-Harpf AE and Deussen DN.

10 weeks after TAC intervention U50-TAC showed more endothelial caveolae than its vehicle treated counterpart. Veh-TAC displayed diminished caveolae formations compared to sham operated animals.

6.2. RNA sequencing

Gene Ratio: The denominator is the number of genes within the list, which are annotated to the GO (Gene Ontology enrichment analysis) of interest. The numerator is the size of the list of genes of interest.

Gene Count: The number of genes within that list which are annotated to the GO of interest.

6.2.1. Veh-Sham vs Veh-TAC

The comparison of vehicle group TAC to group Sham showed a total of 487 up-regulated genes (red) and 201 down-regulated genes (green). The volcano plot (Figure 16) gives an overview of expression fold-change on the X-axis and the p-value on the Y-axis.
The heatmap shows the expression patterns of single animals in the two groups. Veh-Sham in red and Veh-TAC in blue were displaying distinct patterns. With significant alteration in 688 different genes a broad spectrum of functional and mechanistic changes were induced by TAC surgery. KEGG pathway analysis was utilized to group the results and relate them to known pathways.

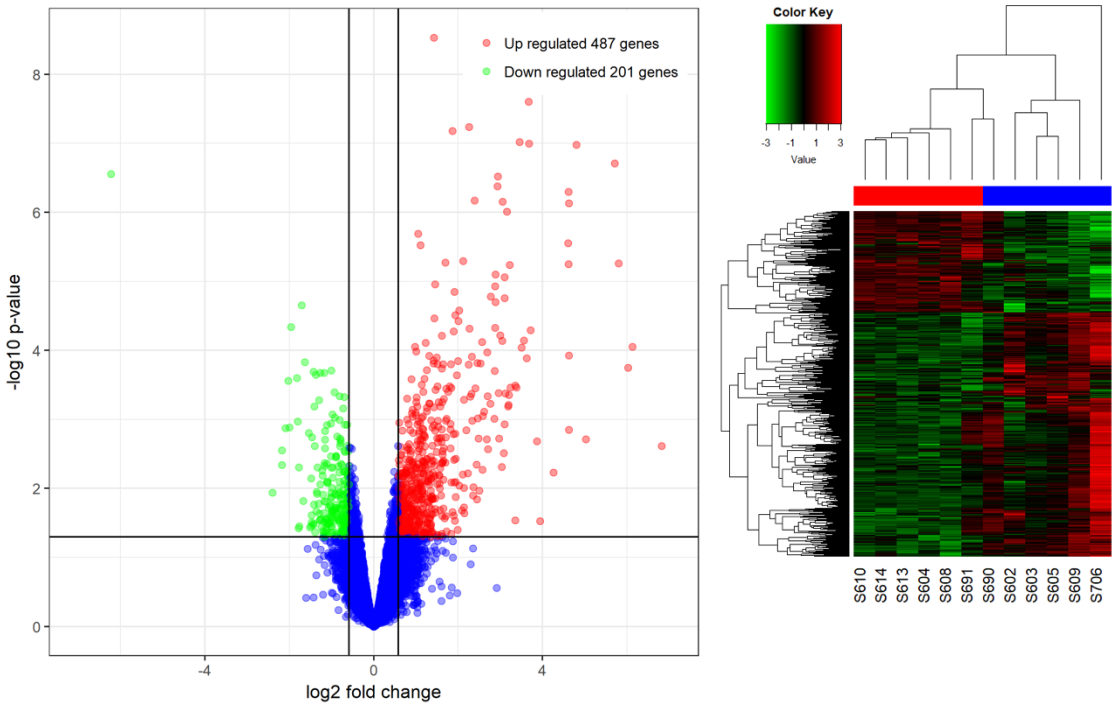

Figure 16: Genes showing altered (up / down) expression with p < 0.05 and more than 1.5-fold changes were considered differentially expressed. Volcano plot of Veh-TAC / Veh-Sham, with group p-value (-log10) on the Y-axis and fold change (log2) on the X-axis. Heatmap of all expression-analyzed single animals in Veh-Sham (red) and Veh-TAC (blue); up-regulated genes in red and downregulated in green.

Expression analysis showed robust alterations in the cellular components. Strongest changes were found in the extracellular matrix and the proteinaceous extracellular matrix, followed by changes of collagen expression and sarcomere levels.

Altered biological processes were angiogenesis, cell growth, ECM organization, changes in circulatory processes and “regulation in the response to wounding including cytosine binding”. Differences of molecular functions were glycosaminoglycan binding, growth factor stimulation, action ECM and collagen binding, just to name a few.

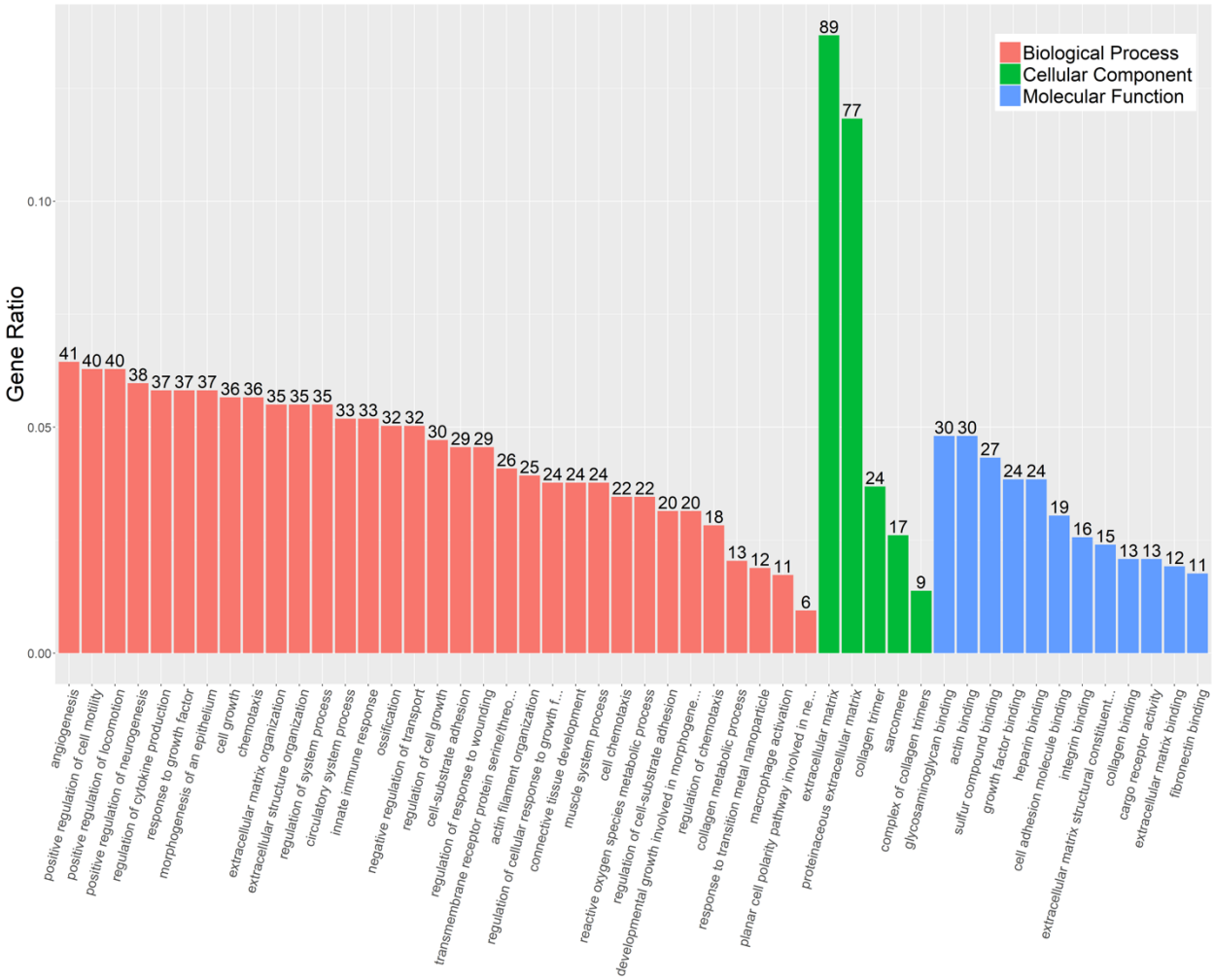

Figure 17: GO enrichment analysis of Veh-TAC and Sham-TAC. Genes presenting altered expression with p < 0.05 and more than 1.5-fold changes were considered differentially expressed. Goseq [101] was utilized to perform the GO enrichment analysis and grouped to distinct biological, cellular or molecular processes. The number above the bars states the amount of altered genes to a specific function.

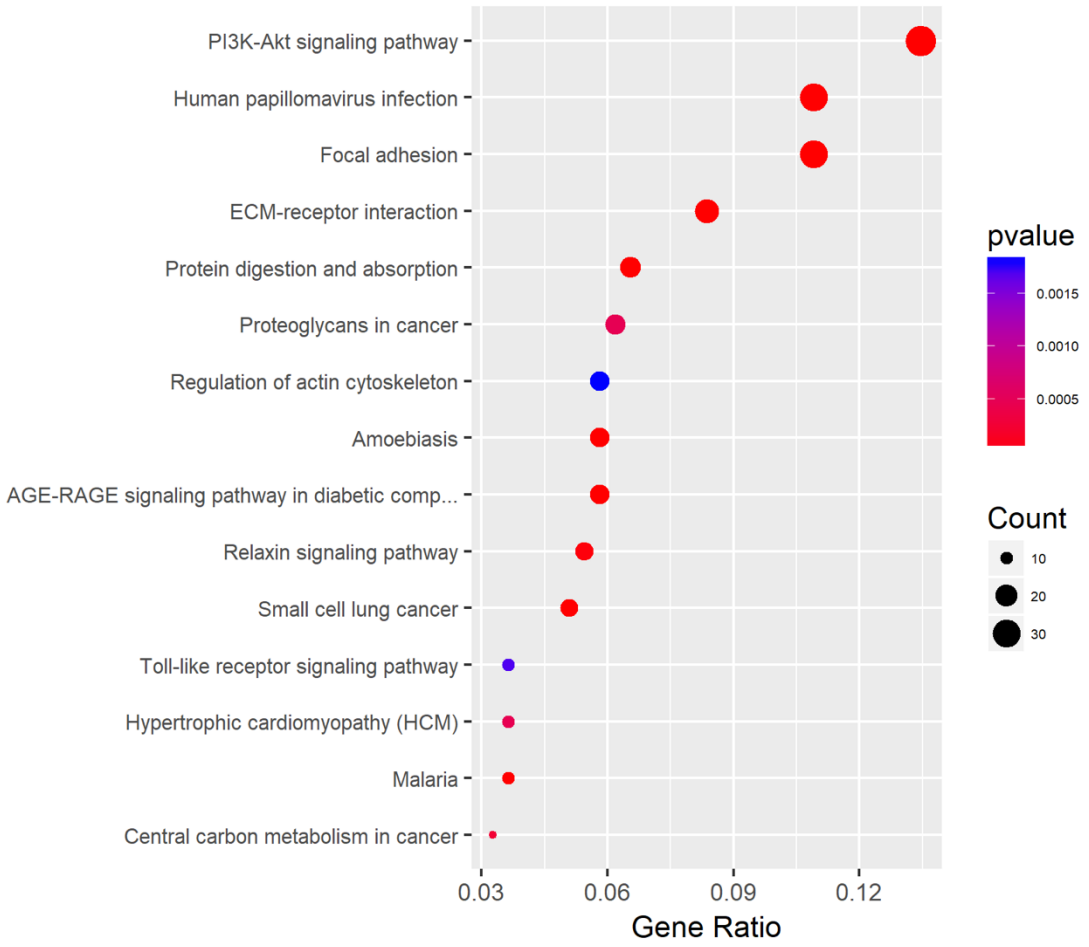

Figure 18: Veh-TAC vs Veh-Sham. The Gene Ratio describes the number of genes within that list which are annotated to the GO of interest. Shading indicates the p-value and circle size accounts for the count of significantly altered genes.

Between Vehicle TAC and Sham the PI3K-Akt signaling pathway is a standout, as it was highly significant ($p < 0.0005$), included the most altered genes (37) and showed the largest changes in expression (Bg. ratio 356/8204).

The pathway “human papilloma virus infection” describes an altered expression of 30 genes (see below), that have been linked to this distinct pathology. Instead of a human papilloma infection, it is a downregulation of Wnt-Fzd signaling and severe changes in collagen expression.
(Cdkn1a/Col1a1/Col1a2/Col4a1/Col4a2/Col4a3/Col4a4/Col6a1/Col6a2/Comp/Creb3l1/Creb3l2/Dvl3/Fn1/Fzd1/Fzd2/Itga11/Itga9/Itgb5/Lama3/Lamb3/Pik3r1/Ptgs2/Reln/Spp1/Thbs1/Thbs3/Thbs4/Tnc/Traf3).

6.2.2. U50-TAC vs Veh-TAC

The differences in expression between U50-TAC and Veh-TAC were less in number. However, both groups have similarities through the adaptations to TAC. When comparing U50-TAC to Veh-TAC only nine upregulated genes were found, together with 45 downregulated genes. The heatmap showed a less distinct profile and a higher interindividual variance (U50-TAC in red, Veh in blue).

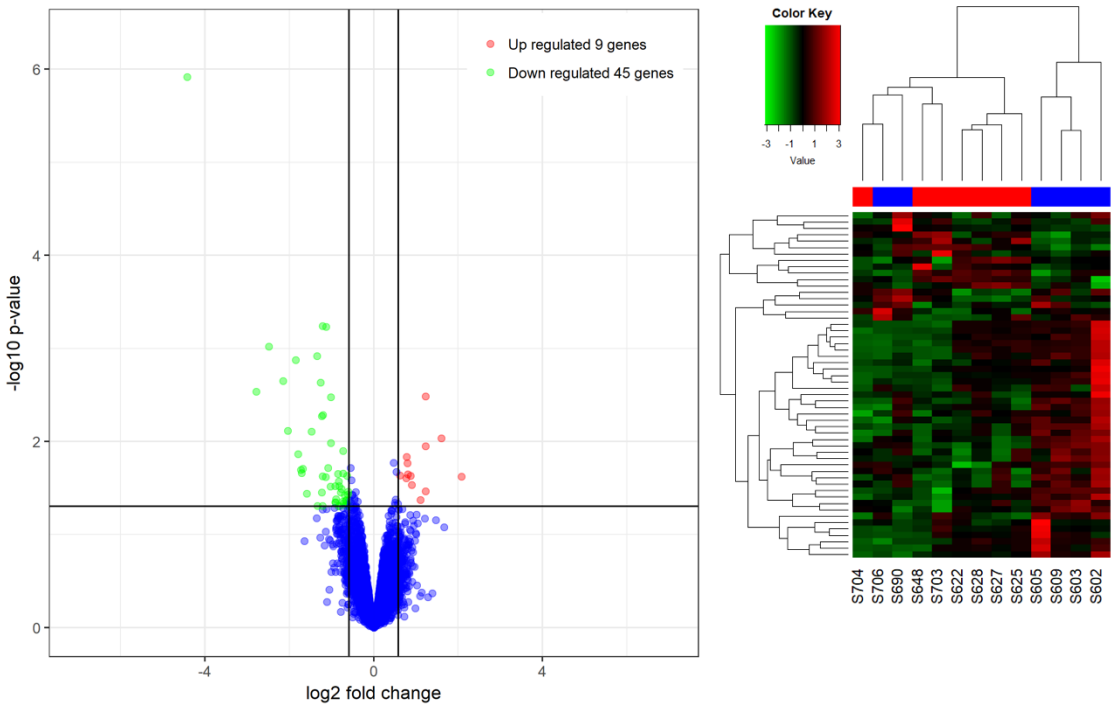

Figure 19: Genes presenting altered expression with p < 0.05 and more than 1.5-fold changes were considered differentially expressed. Volcano plot of U50-TAC / Veh-TAC, with p-value (-log10) on the Y-axis and fold change (log2) on the X-axis. Heatmap of all expression-analyzed single animals in U50-TAC (red) and Veh-TAC (blue); up-regulated genes in red and downregulated in green.

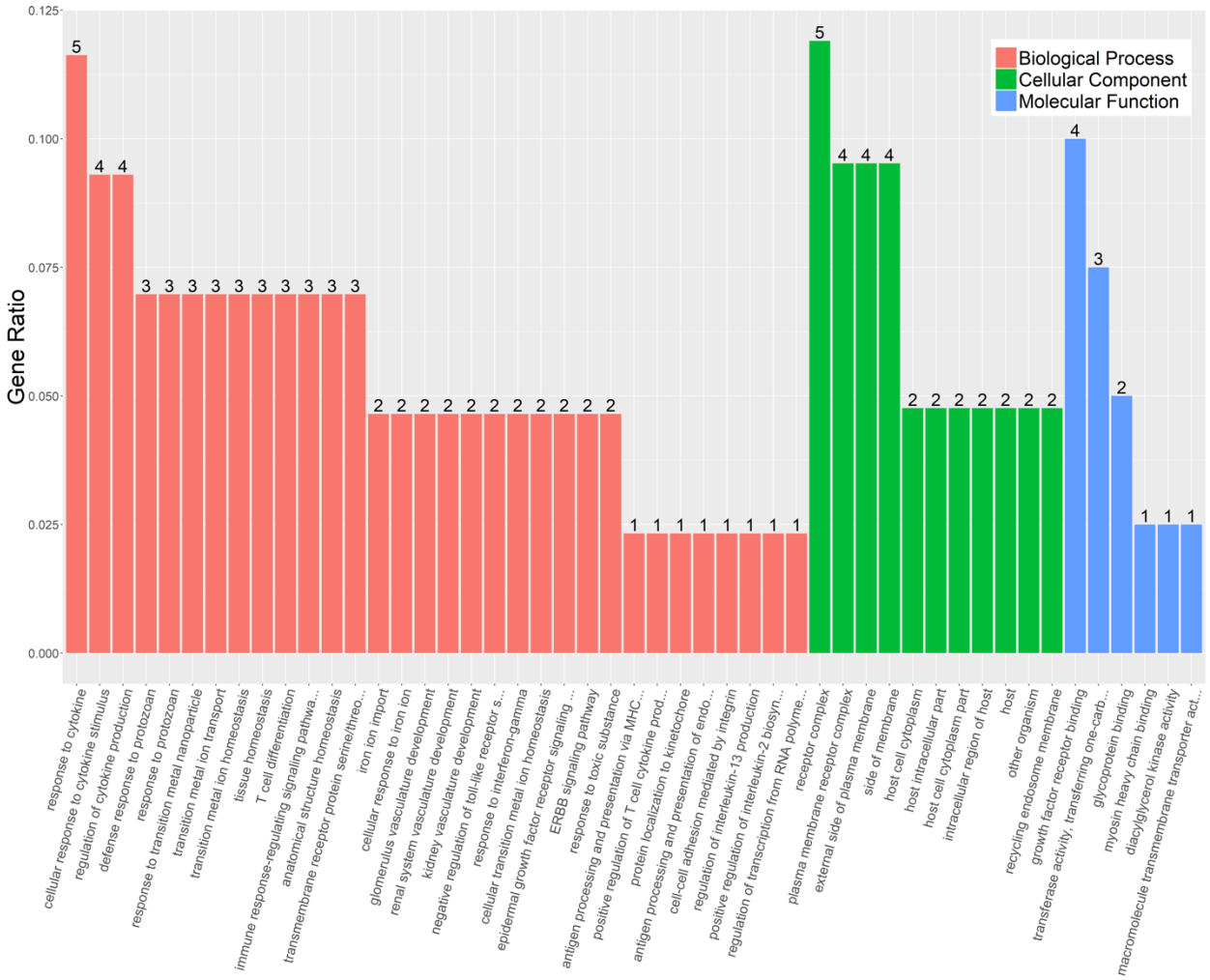

Figure 20: GO enrichment analysis for U50-TAC versus Veh-TAC. Genes presenting altered expression with p < 0.05 and more than 1.5-fold changes were considered differentially expressed. Goseq [101] was utilized to perform the GO enrichment analysis and grouped to distinct biological, cellular or molecular processes. The number above the bars states the amount of altered genes to a specific function.

GO enrichment displays changes in the response to cytokines and their production, growth factor signaling and plasma membrane receptor complex formations.

The KEGG pathway analysis showed three pathways that differed between the groups. First, the apelin signaling pathway ($p < 0.05$) with changes in Egr1 and Myl4 expression. Second, a strong alteration in the HIF-1 signaling pathway ($p < 0.02$) including Angpt2 and Tfrc. And the third pathway detected was Ferroptosis ($p < 0.005$), with significant changes in Slc39a8 and Tfrc expression.

The same three pathways were significantly altered when comparing the U50 TAC group to U50 Sham. The above-mentioned pathways are mapped and interpreted in the discussion (chapter 7.2.).

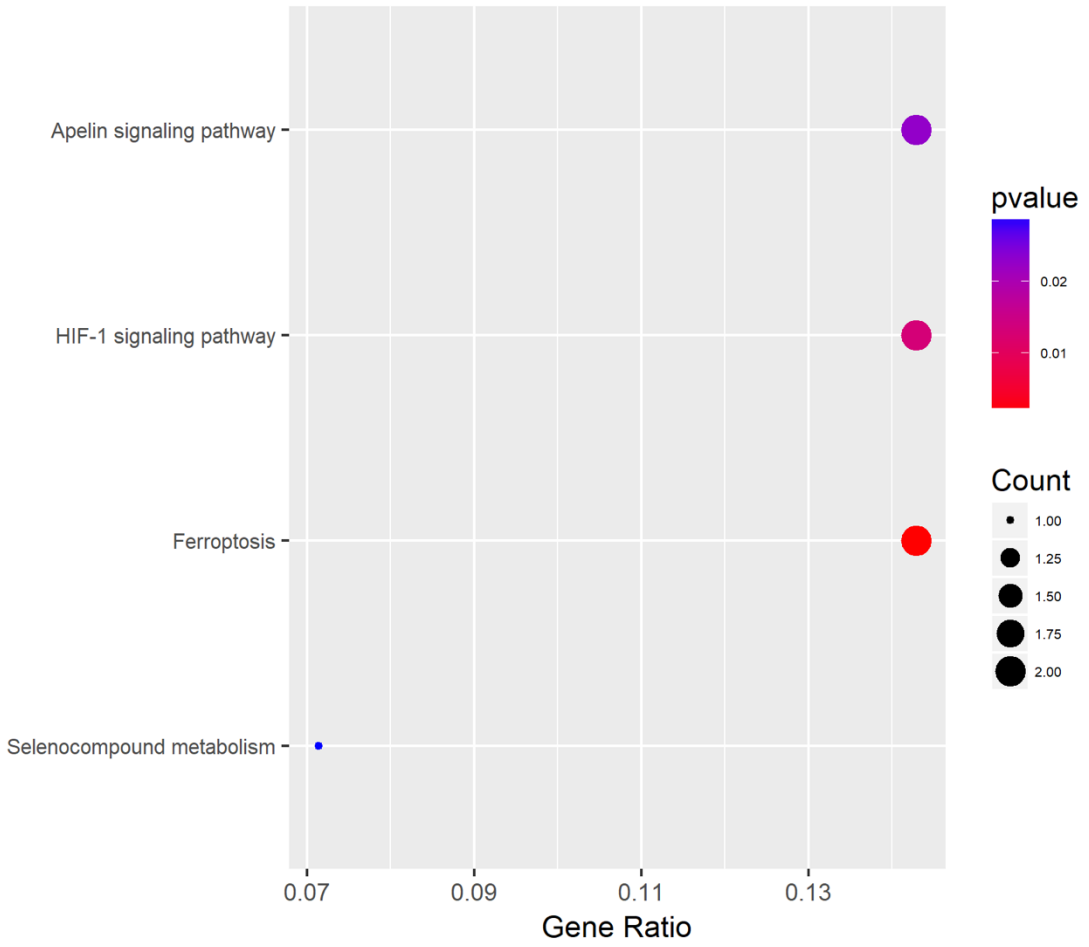

Figure 21: Gene Ratio for U50-TAC vs Veh-TAC. The Gene Ratio describes the number of genes within that list which are annotated to the GO of interest. Shading indicates the p-value and circle size accounts for the count of significantly altered genes.

6.2.3. FIT-TAC vs. Veh-TAC

A total of 23 up-regulated genes and 75 down-regulated genes were found, when comparing the effects of delta ORA treatment versus control (Veh-TAC). An alternate activation pattern was detected especially in PI3K-signaling (Bg ratio 356/8204, $p < 0.005$). Changed gene ratios included downregulated Angpt1/Figf/Gng2/Itga4 and Chrm2/Tnc upregulated in FIT-TAC.

In addition, IL-17 signaling was changed with up-regulations of Ccl2/Lcn2/Mmp3/S100a9 ($p < 0.001$). Further the AGE-RAGE pathway ($p < 0.01$) with Ccl2/F3/Figf was significantly altered.

Interferon related genes and angiopoietin were downregulated in FIT, when compared to Vehicle. These changes are labeled as “basal cell carcinoma” ($p < 0.05$) with downregulation of Wnt2b and Wnt5a.

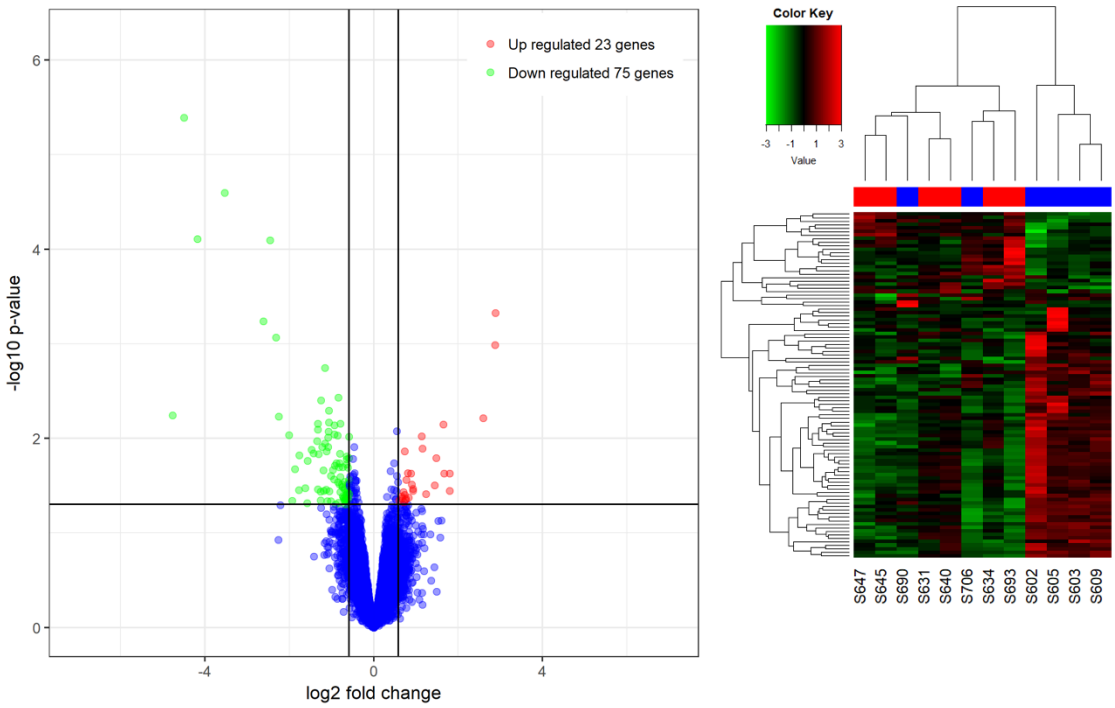

Figure 22: Genes presenting altered expression with p < 0.05 and more than 1.5-fold changes were considered differentially expressed. Volcano plot of FIT-TAC / Veh-TAC, with p-value (-log10) on the Y-axis and fold change (log2) on the X-axis. Heatmap of all expression-analyzed single animals in FIT-TAC (red) and Veh-TAC (blue); up-regulated genes in red and downregulated in green.

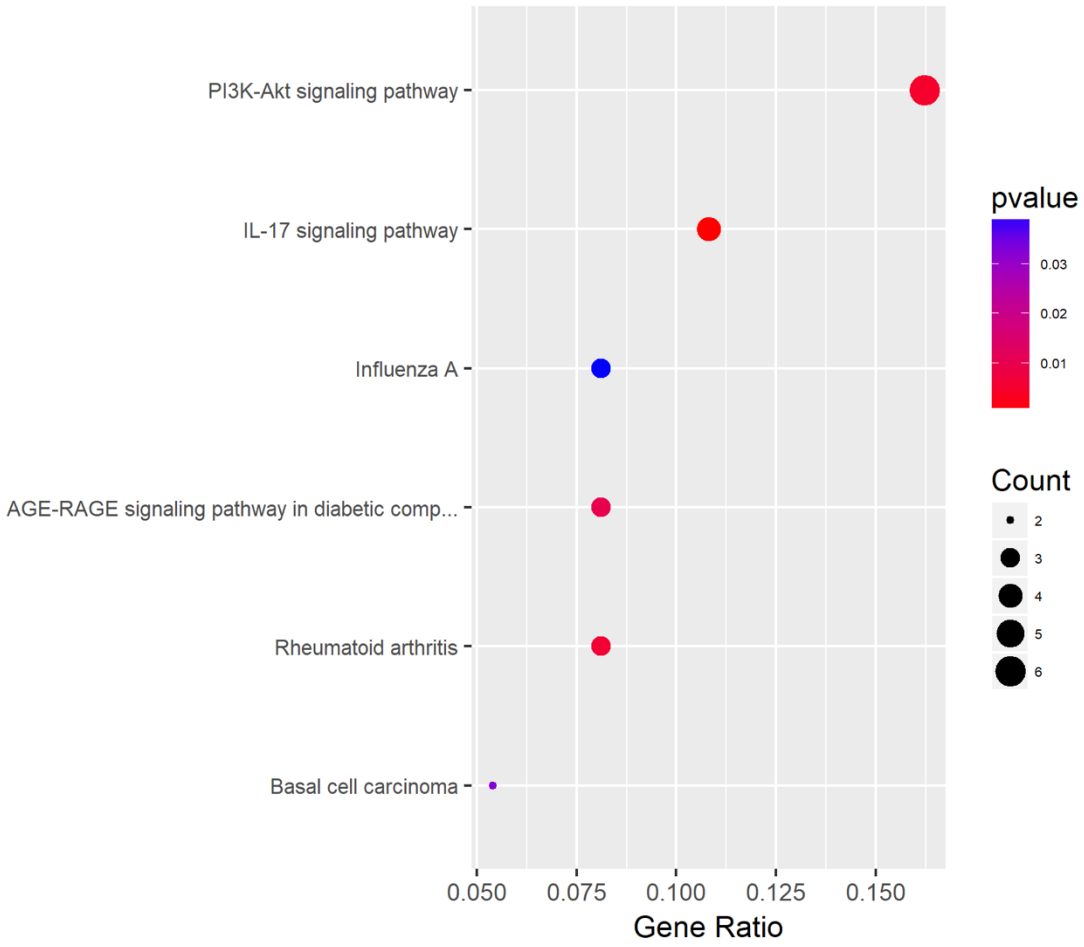

Figure 23: Gene Ratio analysis of FIT-TAC vs. Veh-TAC. The Gene Ratio describes the number of genes within that list which are annotated to the GO of interest. Shading indicates the p-value and circle size accounts for the count of significantly altered genes.

6.2.4. U50-TAC vs FIT-TAC

We detected 11 up-regulated and 47 down-regulated genes when comparing U50-TAC and FIT-TAC. The heatmap demonstrates that the FIT-TAC group in itself has a very heterogeneous expression pattern. With two animals, S634 and S693, showed immense alterations when compared to the rest.

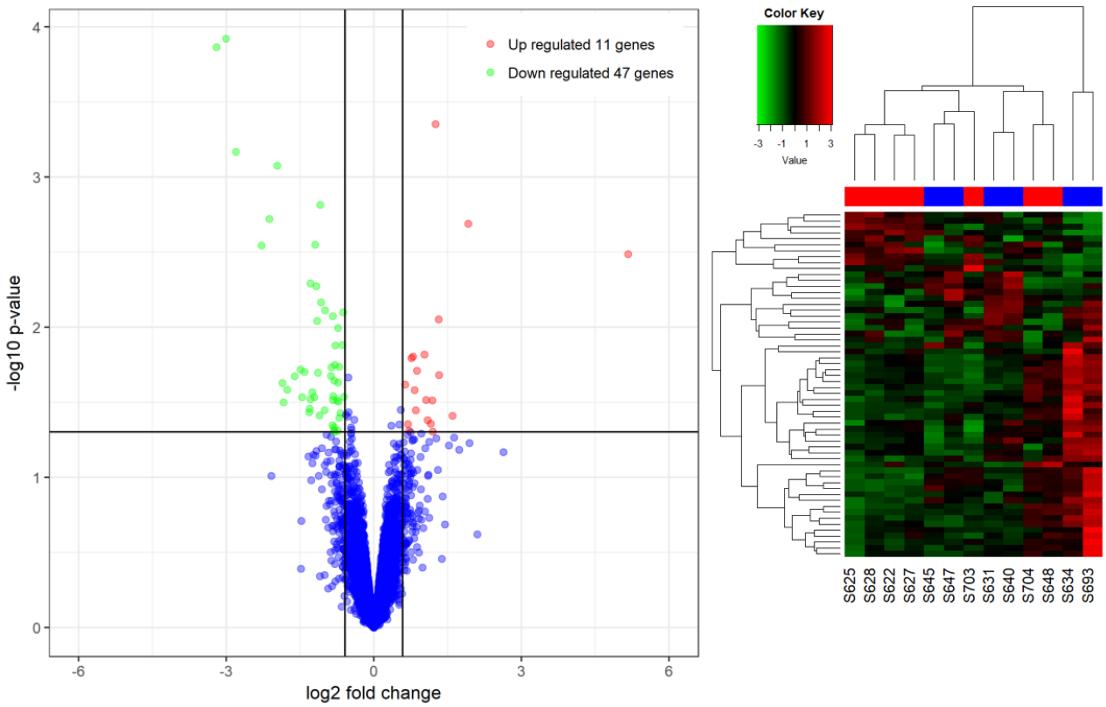

Figure 24: Genes presenting altered expression with p < 0.05 and more than 1.5-fold changes were considered differentially expressed. Volcano plot of U50-TAC / FIT-TAC, with p-value (-log10) on the Y-axis and fold change (log2) on the X-axis. Heatmap of all expression-analyzed single animals in U50-TAC (red) and FIT-TAC (blue); up-regulated genes in red and downregulated in green.

Differences between the two groups were found in angiogenesis, regulation of cell growth, cytokine signaling, MAPK signaling and ECM organization.
The standout pathways were PI3K-Akt / MAPK, HIF-1, cytokine-signaling and ECM-organization.

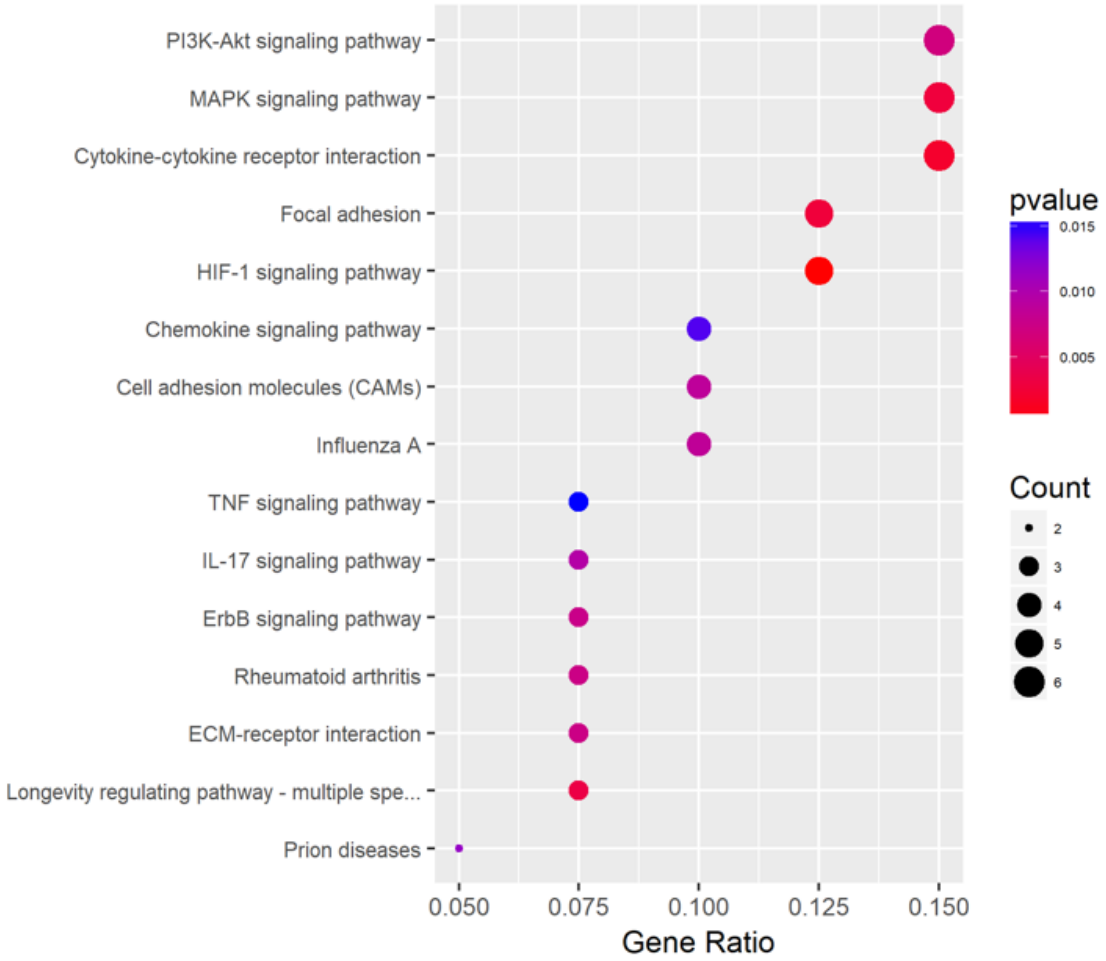

Figure 25: Gene Ratio analysis of U50-TAC and FIT-TAC. The Gene Ratio describes the number of genes within that list which are annotated to the GO of interest. Shading indicates the p-value and circle size accounts for the count of significantly altered genes.

7. Discussion

7.1. Transverse aortic constriction

Vehicle TAC / Vehicle Sham

Pressure overload led to the induction of cardiac hypertrophy, as expected and extensively described in the literature. As evaluated with echocardiography, a significant hypertrophy of the septum and LV posterior wall was already established before treatment start, two weeks after TAC surgery. Hypertrophy increased over the next weeks, in the second half of the study period the average increase was blunted. Between the six- and eight-week time points, half of the group showed %EF well below 40% (24-31%), giving evidence for proceeding towards HF. The other half had ejection fractions above this borderline, but markedly reduced when compared to sham. This half/half split has been reported in earlier publications and can be explained by interindividual differences, slight distinctions in ligation-tightness or probably a combination of both. Further, the discussion of HFrEF vs. HFpEF, as mentioned above, could be resumed here. Interestingly, the Vcf decline was more homogenous in the vehicle group, with all animals dropping below half of the speed measured in sham.

Our RNA-seq data displayed strongest alterations in the PI3K-Akt signaling pathway, when compared to Sham. Dysregulation led to detachment from physiological adaptations. The need for a tight regulation of PI3K-Akt has been found to be essential in homeostasis as well as in functional adaptation [106].

The TAC model showed strong alterations in focal adhesion, ECM and cytoskeleton regulation, known as myocardial remodeling [107]. Changes were solid in Wnt-signaling, known for its role in regulation of fibroblasts, collagen-formation and synthesis. The role of the Wnt-Frizzled (Fzd) GPCR complex has been studied in hypertrophy and fibrosis, in the development of MI and arrhythmias and HF progression [108] [109]. Wnt signaling is quiescent in adult myocytes [109] [110] but becomes reactivated in pressure overload induced hypertrophy [111]. Since 2010, interactions of Wnt-Fzd and opioid receptors have been described, primarily with the mu OR. In preliminary experiments our laboratory has seen, that the at least partly Wnt regulated connexin43 (Cx43) expression was reduced in TAC, but not in ORA treated TAC. Wnt dependent Cx43 expression has been linked to regulation of myocardial electrical stability and maintained heart function [112]. Stronger activation of the AGE-RAGE pathway (advanced glycation end products) presented evidence for an increased amount of reactive oxygen species, inflammation and dysregulations in energy homeostasis [113].

Since the new millennium, studies utilized microarrays to look deeper into hypertrophic regulation, avoiding bias and with the chance to cluster gene-groups. Kong *et al.* [114] compared an exercise hypertrophy group to a sedentary group (Dahl salt-sensitive rats on low-salt diet) and a set of Dahl salt-sensitive rats on high-salt diet (develop pathologic hypertrophy). The fourth group was a prolonged high salt diet, that progressed into heart failure (decompensated hypertrophy). The microarray (Affimetrix Rat Genome U34A) compared about 3000 genes, from which about 400 were altered in one or more of the tested groups. In physiological hypertrophy these genes were regulating metabolism and cell growth, for example the IGF/EGF signaling pathway. Whereas pathological hypertrophy was associated with genes clustered for inflammation and cellular stress. Common activation of both types were genes involved in cell growth, as shown in figure 26. The decompensated/HF group showed a similar, but stronger activation of the clusters seen in pathological hypertrophy and additionally included apoptotic factors.
The above-mentioned mediators were confirmed to be of relevance by a group comparing treadmill induced hypertrophy to maladaptive hypertrophy. In the exercise group no upregulation of fetal genes, ANP or BNP was observed. Further markers of derangement, including actin/myosin derailment, increased collagen expression or fibrosis marker, could only be detected in pathological development [115].

In physiological hypertrophy, insulin-like growth factor 1 (IGF1) acts via the IGF1 receptor and activates downstream phosphoinositide-3 kinase (PI3-K), Akt1 and later downstream the mammalian target of rapamycin (mTOR) and the ribosomal S6 kinases (S6K) [106]. IGF1 upregulations have been measured in athletes as well as patients with HCM [116] [117]. In pathological hypertrophy a $G_{\alpha q}$-PLC_b-PKC activation has been described, triggered by factors as noradrenaline, angiotensin II and endothelin (ET)-1 [106].

With our TAC control group, we were able to replicate a well described phenotype and show the validity of our model. Alterations in energy metabolism, heart structure and increased stress were evident. With 89 significantly altered reads ECM remodeling and changes in proteinaceous-ECM (77) were standouts in the GO's cellular compartment. Important biological processes found in 10wk post TAC were angiogenesis (41), cytokine production (37) and cell growth (36).

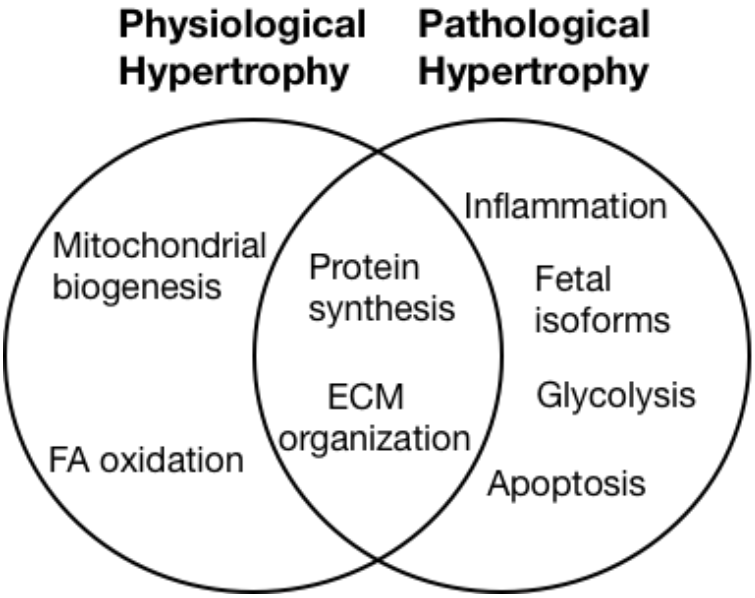

Figure 26: Physiological and pathological hypertrophy; adapted from DornII *et al.* 2007. By DN Deussen.

7.2. KORA - U50 treatment

U50 treatment was beneficial in pressure overload exposed mice.
After prolonged KORA treatment, we saw preserved heart function following TAC. The magnitude of the hypertrophic response, following the ligation, was comparable to those of vehicle and DORA treated animals. Heart weight/tibia length and extent of hypertrophy measured by echocardiography were not different between the TAC groups. This suggests that KORA does not reduce hypertrophy per se but may be impacting molecular mechanisms that improve heart function. A prevention of hypertrophy has been only described when isoproterenol (stimulus) and U50 (treatment) where administered simultaneously [85] [86]. In a study comparing rat heart hypertrophy, induced either by swimming exercise or spontaneous hypertension, a similar extent of hypertrophy was found in both regimes. But only the hypertensive group displayed an upregulation of neurohumoral pathways, translating the mechanical stress into pathological growth. Including angiotensin converting enzyme (ACE), brain natriuretic peptide (BNP), beta-adrenergic receptor kinase and the endothelin receptor [118].

The heart function of the KORA TAC animals did not decrease as observed in the vehicle-treated TAC mice. Importantly at eight weeks after TAC, six out of the seven U50-treated TAC animals showed no significant reduction in EF and FS, when compared to the sham groups. After ten weeks the mean EF showed a slight downward trend. The only outlier

displayed functional measurements comparable to those of the control group, with an EF of 31.5% and an FS of 14.8%. Six of the seven animals benefited significantly from KORA treatment and maintained functionality, while LV hypertrophy remained unchanged.
Previous research compared mice exposed to pressure overload induced hypertrophy by TAC for one week, to a group of mice, subjected to four weeks of chronic swim exercise-training. Both regimes resulted in cardiac hypertrophy, but with a significant difference in cardiac morphology. For instance, an increase in interstitial fibrosis has been found only in the TAC animals and not in the exercise group [119]. Interstitial and perivascular fibrosis is a morphologic hallmark of different functional myocardial pathologies. The accumulation of cardiac fibroblasts and extracellular matrix proteins creates mechanical stiffness and, in this way, reduces the function of the heart. Furthermore the occurrence of collagen-rich regions in the heart causes disruption of excitation-contraction coupling between the myocytes, intensifying the reduction in cardiac contractility [120]. These findings go alongside with our structural findings in TEM and histology described above in chapter 6.1. In electron microscopy imaging mitochondrial integrity was preserved in U50-TAC when compared to vehicle TAC. Recently a KOR activation has been linked to mitochondrial fusion and thus delivering mitochondrial resistance to IR-injury in cardiomyocytes [121].

To investigate the mechanism underlying the favored adaptation in our ORA treated mice we utilized an RNA sequencing approach on left ventricular tissue. When looking at the expression patterns of U50-treated TAC and vehicle-treated TAC there are far more commonalities than differences. Cell growth, structural reorganization and changed PI3K signaling seem to be induced by TAC surgery, but microscopy showed a structural advantage in U50 treated TAC. With the RNA sequencing, distinctions were identified in three mayor pathways: apelin signaling, HIF-1 signaling and iron handling, a response that was selective to K-ORA treatment only.

HIF-1α
A decreased HIF-1α has been described in both aging and Hif1α $^{+/-}$-mice [122]. The reduction in HIF-1α came alongside with lowered expression of VEGF, ANGPT1, ANGPT2, PGF and other angiogenic growth factors. In our model, we also observed a distinctive regulation of this axis when comparing the U50-treated TAC to controls. As described above, the tight regulation of vascularization goes hand in hand with the function of the challenged heart. From our data we cannot conclude whether these changes are creating the phenotype we are seeing, or if we only observe the results of earlier adaptations in structure and vascularization. But the significantly higher expression

of above mentioned ANGPT2 in Veh-TAC and FIT-TAC provides further evidence of a beneficial prognosis for U50 treatment in HF. In chronic HF patients ANGPT2 showed its potential as a biomarker for the predictive one-year outcome, similar to pro-BNP [123].

HIF-1α deficient mice develop rapid HF with massive LV hypertrophy after TAC surgery and are unable to regulate neovascularization and to maintain oxygen homeostasis [124]. Pathways of HIF regulation have been described through transforming growth factor-β (TGF-β) via the canonical pathway through Smad2/3 and the non-canonical pathway through MAPK (ERK1/2) [125]. Here, too, we see alterations between our groups, especially when comparing KORA and DORA TAC. It seems that a tight regulation is essential to maintain functionality and over- or underpowered pathway-activity is led to a loss of function.

From data of a MI-injury model (LAD), Tong *et al.* proposed that the protective properties of U50,488H were mediated through heme-oxygenase-1 (HO-1) via the PI3K-Akt-Nrf2 pathway [73]. The regulation of KOR expression under hypoxia via HIF-1 has been previously described [126]. HIF-1 is further involved in iron metabolism, linking this alteration to the enhanced expression of genes involved in iron homeostasis. This fits into the picture of enhanced O_2 supply and thus higher contractile potential in U50 treated TAC. Iron depletion on the other hand has been described in HF, 'linking' anemia and adverse prognosis [127].

HIF-1 regulates mitochondrial mass, as well as metabolism in the heart, distributing resources and adapting to changing environments [128]. The regulation of HIF-1 has been further linked to the protective effects of IPC of the heart [129].

HIF Pathway

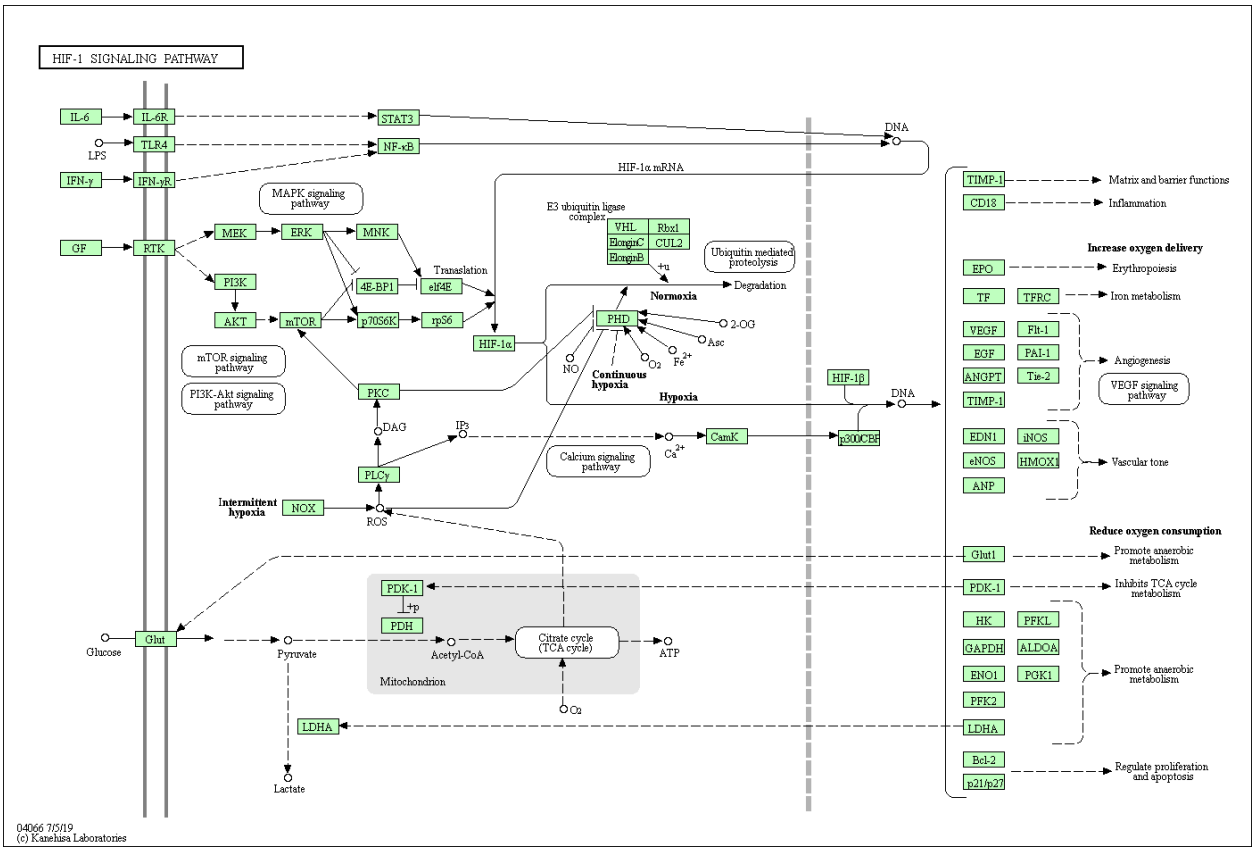

Figure 27: HIF-1 signaling pathway - Homo sapiens (human), copied on 22.10.2020 from: https://www.genome.jp/kegg-bin/show_pathway?hsa04066

Apelin

To our knowledge we are the first to demonstrate KORA treatment influences the apelin axis in heart failure. This provides further evidence for interactions of different GPCR's in the regulation of myocyte homeostasis, here in particular APL and KOR. As mentioned above, apelin has been described to regulate KOR [130] [131]. Here we see first evidence that this might work in both ways.

Alterations in apelin-pathway-signaling appear to be one of the main protective factors that make the difference between the well performing KORA treated hearts and the diminishing cardiac performance in the control group.

The apelin receptor itself is a seven transmembrane domain GPCR, with apelin as its only known ligand. APJ has been found to be highly altered in left ventricle specimen from heart failure patients [132]. For the apelin pathway, vasoconstrictive, as well as vasodilative effects, have been described depending on the model and utilized concentrations [133] [134]. In cultured endothelial-cells, hypoxia provoked an upregulation of apelin mRNA and protein levels, induced by the HIF pathway [135].

Interestingly, expression of apelin and APJ were both induced by endurance exercise in heart and vasculature. Sedentary spontaneous hypertensive rats (SHR) had significantly lower apelin/APJ activity when compared to swim-trained SHR's. Exercised rats showed lower systolic blood pressure and BNP-mRNA but displayed no difference in myocyte size. The data suggests that the apelin pathway may be involved in the positive effects of exercise regimes on hypertension. Endurance training was able to maintain function, showed superior clinical biomarkers, but did not reduce already established hypertrophy [136]. In our study, pathological development seems to be disrupted and the hearts maintain functionality, suggesting the potential for opioid receptor stimulation in cross activation of physiological hypertrophy pathways. Our data contributes to the understanding of this obviously important axis in cardiac regulation.

In a study by Rostamzadeh *et al.,* apelin reduced mean arterial pressure and increased contractile function in renovascular hypertensive rats (2K1C). The apelin effect was achieved by a normalization of apelin receptor (APJ)-KOR heterodimerization [131] [137]. This heterodimerization through apelin treatment attenuated the elevated KOR response that was induced by hypertension. Through the "fine-tuning" of APJ-KOR, a beneficial recovery of ERK1/2 phosphorylation was accomplished. In a follow-up study by the same group the pathway activation and consequently the outcome strongly depended on the magnitude of the apelin stimulation [133].

In ageing, reduced levels of endogenous apelin have been described in humans and rodents [138]. The authors reported that muscle contraction induced apelin expression and the release into circulation. This capacity is reduced in aging and sarcopenia. With pharmacological apelin-based interventions, the group was able to enhance muscle function through mitochondriogenesis, anti-inflammatory signaling and regulation of autophagy.

Apelin pathway

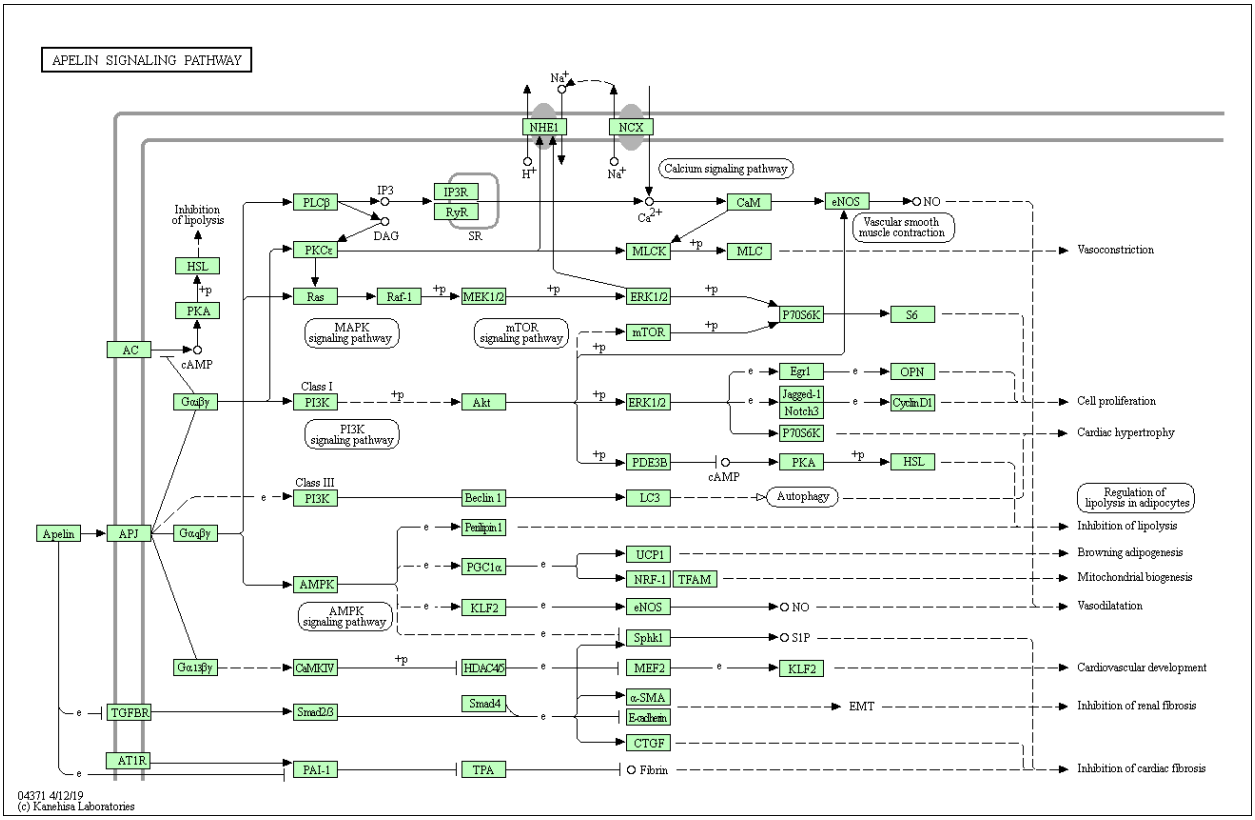

Figure 28: KEGG Apelin signaling pathway - Homo sapiens (human), copied on 22.10.2020 from:https://www.genome.jp/kegg-bin/show_pathway?map=hsa04371&show_description=show

Transmission electron microscopy of hearts from U50-TAC further showed increased numbers of caveolae in the endothelium. Migration of caveolin towards mitochondria has been described as an adaption to cellular stress in the heart [139] [140]. The increased caveolae formation could be of advantage when it comes to energy supply of the enlarged hearts. A KOR colocalization with Cav 1.2 has been described in rat heart [141].

Apelin, HIF-1a, and caveolae formation have all been linked to stress adaptation in the heart [142] [143] [139]. These signaling pathways regulate neovascularization [144] [145], vascular tone [146] [147] [134] and energy metabolism in cardiovascular tissue [148] [149] and may account for the preservation and improvement in cardiac function we observed with kappa opioid receptor activation in the TAC model. As described above, the changes we noticed in U50 treated mice have been linked to exercise induced adaptation, combined with a higher cardiac capacity. This may justify the assumption that KORA stimulation has exercise mimicking effects.

All these recent findings together with our experiments support a central role of the HIF-1/Apelin/KOR axis in cardiac protection. Interestingly, all of the mentioned mediators seem to be highly involved in physiological adaptation of the heart. This axis therefore appears an attractive target for future cardiovascular drug development and disease modification. Especially KORA might offer a new treatment toward enhanced heart function that is based on physiological remodeling in the setting of pathophysiology.
Nalfurafine hydrochloride, a selective and potent KORA, has been found save to patients in clinical trials, as i.v. and oral administration. The drug is KOR-specific and is currently prescribed in Japan for pruritus treatment in patients with kidney disease or chronic liver disease [150]. Safety data from real life clinical experience and the pathophysiologic rational outlined above could help to fast-track pre-clinical studies on nalfurafine in other countries and other diseases, especially HF [151] [152].

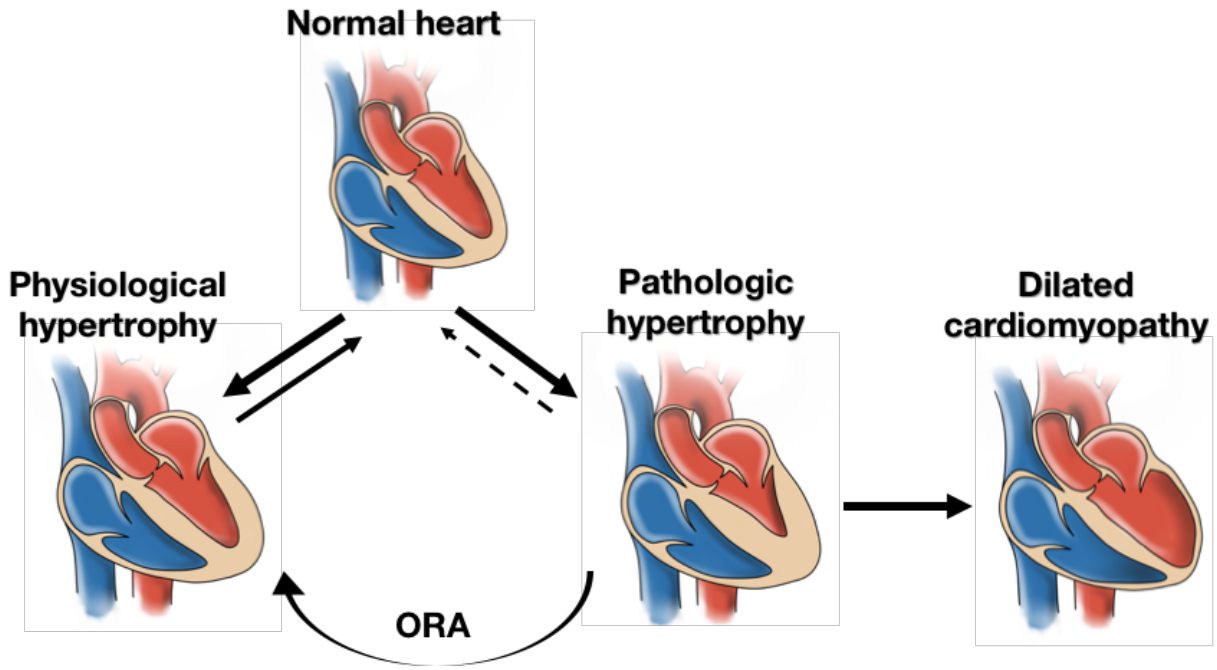

Figure 29: Hypertrophic response of the heart. When looking at our initial hypothesis we can state that we were able to shift the pathologic hypertrophy towards a more physiologically functioning adaptation with an exogenic opioid kappa receptor agonist. Figure by Huebner T & Deussen DN.

7.3. DORA - FIT treatment

The hypertrophic response in FIT-TAC did not differ from the other groups. In functorial measurements DOR agonism stayed behind our expectations initiated through earlier results on this topic, especially cardiac protection against I/R injury [79] [153]. Patel *et al.* demonstrated a co-localization of Cav-3 and DOR in protection of myocytes from ischemic damage. Results in a LAD-dog model, showed that DOR and ROS signaling were obligatory for IPC induced reduction in infarct size and arrhythmic events [80]. Further, at least partially exercise induced cardio protection has been linked to DOR activation [72]. In a rat exercise plus MI model a pharmacological blockade of DOR abolished the exercise induced reduction in infarct size.

Results of the echocardiography showed a split in our DORA group starting at treatment week two (4wk post TAC) and this trend continued until the endpoint measurement. Here three animals showed an EF between 24% and 42% and the other four between 54% and 77%. Some animals were performing not worse than the Sham or U50-TAC, but some were already on the path towards HF. We can only speculate that possibly the dose (p.24) applied was just on the verge of the therapeutic margin needed to treat. Hence, only some animals appeared to benefit from DORA treatment, with preserved heart function after 10 weeks of TAC.

The heterogenous response rendered the interpretation of the RNA-seq data prone to error, since some animals were already showing signs of HF and others were still performing well. Thus, it will be necessary to distinguish the differences within the FIT-TAC group, before comparing it to the other treatment groups. DORA treatment in cardiovascular diseases has shown promising results, as discussed in chapter 3.3.3., but in the dosage we tested, the delta opioid agonist FIT was not able to induce similar favorable effects as the above discussed KORA.

7.4. Limitations

The RNA sequencing results of our model linked together KOR-HIF-1-Angpt2-MAPK-PI3K-Apelin in the adaptation to pressure overload induced LV hypertrophy for the first time. This shows not only how valuable sequencing approaches are, but also how limited the understanding of the myocardial response to stress and its finetuned adjustments still is. We need novel algorithms and integrated models to analyze the new “flood of data” and see that one pathway is not independent from another, getting closer to the complexity in vivo [154] [155].

Our study investigated the long-term physiological function together with the RNA expression patterns at a late point in the disease model. It would be of great interest to

see the dividing factors of ORA and vehicle treated animals immediately after treatment start. Transcription differences might be detectable already hours to days after drug administration. Identifying these early players could help to understand and utilize ORAs and pave the way to long lasting cardiac protection. Our study has shown a beneficial effect by early and continuous treatment in pressure overload challenged hearts. For the future it would be interesting, if a substitution preceding pathological adaptation might offer cardiac protection. To clarify these issues, we already started working with a cell model to further study the early timepoint changes. Therefore, we utilized C2C12 (mouse myoblasts) and H9C2 (rat neonatal cardiomyoblasts) cell cultures and induced hypertrophy with isoprenaline. In this way we will be able to study the immediate changes that the ORA treatment induces. With the results of two different cell lines, we aim to support our *in vivo* results and get closer to the cardioprotective mechanisms behind opioid receptor signaling. Utilizing the cell culture approach, we further want to detect the pathways that the KORA triggers in contrast to DORA. Additionally, we wish to answer if the KORA effects were specific in our model or if the DORA was just underdosed. With the above-mentioned promising effects of DORA in ischemia reperfusion injury we want to investigate this closer before discarding DORA treatment as a possible future drug treatment in heart failure.

A potential limitation is the homogeneous population of only male mice. As long-term clinical observations and recent research indicates, it may be misleading to extrapolate the effects to the opposite sex [156] [157]. But as a starting point, we wanted to compare our results to earlier studies on the topic, that were almost exclusively executed with male laboratory animals. Already in 1994, the US National Institutes of Health (NIH) published a guideline for the study of sex-difference in medical research and 2014 the directors of the NIH specified it to aim for “balanced sex in cell and animal studies” [158]. The U.S. Government Accountability Office has reported that eight out of ten withdrawals of approved drugs have been related to the greater health risks and adverse events for women [159]. This causes great health risks for more than half of our population as well as great costs for the healthcare systems, which could and should be halted in the future by including gender-equality in research.

8. Conclusion

Heart failure is a global health issue and endpoint of different cardiovascular diseases.
Models of pulmonary artery hypertension and myocardial reperfusion-injury have shown beneficial effects of treatment with opioid receptor agonists.
We were able to show that ORA administration has protective long-term effects on heart function in pressure overload induced LV hypertrophy in mice. Kappa opioid receptor activation after TAC was able to maintain contractility and fraction shortening, comparable to sham-operated animals. The TAC induced hypertrophic response of the heart was not reversed by ORA treatment, but function was maintained. A treatment start, after cardiac hypertrophy has already been manifested, mimics the real-life situation of patients with CVDs.
The positive effect that endogenous opioids accomplish in exercise adaptation was achieved in this study with the KORA U50,488H, counteracting the stressful stimuli and preventing diminishing function. Delta opioid agonism (FIT) showed a more diverse effect, with part of the group benefiting from treatment and others failing comparable to vehicle treated TAC.
Transmission electron microscopy revealed preserved myocardial structural integrity and enhanced endothelial caveolae formation in the U50 TAC, indicating plausible mechanism for enhanced functionality.
According to the RNA-sequencing results, the apelin and HIF-1 pathways might play a role in the functional advantage of KORA. From our data at 10wk endpoint we cannot conclude what were the initial drivers of this favorable shift toward preserved function. These promising results should encourage further research on the beneficial effects of opioid receptor stimulation and highlights that exercise associated effects in myocardium may reveal new protective mechanisms.
Based on our results, KORA treatment might offer a new treatment option in pressure overload triggered pathologic cardiac hypertrophy by inducing “exercise-like” adaptations. With a safe and potent KORA (nalfurafine hydrochlorid) available, the chances are high that KORA treatment in heart failure can be tested in clinical trials in the foreseeable future. This could offer patients and clinicians new opportunities to preserve physical performance.

9. References

1 Virani, S. S. *et al.* Heart Disease and Stroke Statistics-2020 Update: A Report From the American Heart Association. *Circulation* **141**, e139-e596, doi:10.1161/cir.0000000000000757 (2020).

2 Timmis, A. *et al.* European Society of Cardiology: cardiovascular disease statistics 2017. *European heart journal* **39**, 508-579 (2017).

3 Mozaffarian, D. *et al.* Heart Disease and Stroke Statistics-2016 Update: A Report From the American Heart Association. *Circulation* **133**, e38 (2016).

4 Tessler, J. & Bordoni, B. in *StatPearls [Internet]* (StatPearls Publishing, 2019).

5 Guha, K. & McDonagh, T. Heart failure epidemiology: European perspective. *Current cardiology reviews* **9**, 123-127 (2013).

6 Ponikowski, P. *et al.* 2016 ESC Guidelines for the diagnosis and treatment of acute and chronic heart failure: The Task Force for the diagnosis and treatment of acute and chronic heart failure of the European Society of Cardiology (ESC)Developed with the special contribution of the Heart Failure Association (HFA) of the ESC. *Eur Heart J* **37**, 2129-2200, doi:10.1093/eurheartj/ehw128 (2016).

7 Burchfield, J. S., Xie, M. & Hill, J. A. Pathological ventricular remodeling: mechanisms: part 1 of 2. *Circulation* **128**, 388-400 (2013).

8 Doenst, T., Nguyen, T. D. & Abel, E. D. Cardiac metabolism in heart failure: implications beyond ATP production. *Circulation research* **113**, 709-724 (2013).

9 Yusuf, S., Pitt, B., Davis, C. E., Hood, W. B., Jr. & Cohn, J. N. Effect of enalapril on mortality and the development of heart failure in asymptomatic patients with reduced left ventricular ejection fractions. *The New England journal of medicine* **327**, 685-691, doi:10.1056/nejm199209033271003 (1992).

10 Russell, S. D. *et al.* New York Heart Association functional class predicts exercise parameters in the current era. *American heart journal* **158**, S24-S30 (2009).

11 McMurray, J. J. *et al.* ESC Guidelines for the diagnosis and treatment of acute and chronic heart failure 2012: The Task Force for the Diagnosis and Treatment of Acute and Chronic Heart Failure 2012 of the European Society of Cardiology. Developed in collaboration with the Heart Failure Association (HFA) of the ESC. *European journal of heart failure* **14**, 803-869 (2012).

12 Rickenbacher, P. *et al.* Heart failure with mid-range ejection fraction: a distinct clinical entity? Insights from the Trial of Intensified versus standard Medical therapy in Elderly patients with Congestive Heart Failure (TIME-CHF). *European journal of heart failure* **19**, 1586-1596 (2017).

13 Vasan, R. S. *et al.* Epidemiology of left ventricular systolic dysfunction and heart failure in the Framingham study: an echocardiographic study over 3 decades. *JACC: Cardiovascular Imaging* **11**, 1-11 (2018).

14 Borlaug, B. A. The pathophysiology of heart failure with preserved ejection fraction. *Nature Reviews Cardiology* **11**, 507 (2014).

15 McKee, P. A., Castelli, W. P., McNamara, P. M. & Kannel, W. B. The natural history of congestive heart failure: the Framingham study. *New England Journal of Medicine* **285**, 1441-1446 (1971).

16 Nieminen, M. S. *et al.* EuroHeart Failure Survey II (EHFS II): a survey on hospitalized acute heart failure patients: description of population. *European heart journal* **27**, 2725-2736 (2006).

17 Rossignol, P., Hernandez, A. F., Solomon, S. D. & Zannad, F. Heart failure drug treatment. *Lancet* **393**, 1034-1044, doi:10.1016/S0140-6736(18)31808-7 (2019).

18 Lang, C. C. & Struthers, A. D. Targeting the renin-angiotensin-aldosterone system in heart failure. *Nat Rev Cardiol* **10**, 125-134, doi:10.1038/nrcardio.2012.196 (2013).

19 Nakamura, M. & Sadoshima, J. Mechanisms of physiological and pathological cardiac hypertrophy. *Nature Reviews Cardiology*, 1 (2018).

20 Shimizu, I. & Minamino, T. Physiological and pathological cardiac hypertrophy. *J Mol Cell Cardiol* **97**, 245-262, doi:10.1016/j.yjmcc.2016.06.001 (2016).

21 Lyon, R. C., Zanella, F., Omens, J. H. & Sheikh, F. Mechanotransduction in cardiac hypertrophy and failure. *Circulation research* **116**, 1462-1476 (2015).

22 McCain, M. L. & Parker, K. K. Mechanotransduction: the role of mechanical stress, myocyte shape, and cytoskeletal architecture on cardiac function. *Pflügers Archiv-European Journal of Physiology* **462**, 89 (2011).

23 Kim, J.-C., Son, M.-J. & Woo, S.-H. Regulation of cardiac calcium by mechanotransduction: Role of mitochondria. *Archives of biochemistry and biophysics* (2018).

24 Mirsky, I. Left ventricular stresses in the intact human heart. *Biophysical journal* **9**, 189-208 (1969).

25 Weeks, K. L. & McMullen, J. R. The athlete's heart vs. the failing heart: can signaling explain the two distinct outcomes? *Physiology (Bethesda, Md.)* **26**, 97-105, doi:10.1152/physiol.00043.2010 (2011).

26 Ekblom, B. & Hermansen, L. Cardiac output in athletes. *Journal of Applied Physiology* **25**, 619-625 (1968).

27 Chapman, C. B., Fisher, J. N. & Sproule, B. J. Behavior of stroke volume at rest and during exercise in human beings. *The Journal of clinical investigation* **39**, 1208-1213 (1960).

28 MacDougall, J., Tuxen, D., Sale, D., Moroz, J. & Sutton, J. Arterial blood pressure response to heavy resistance exercise. *Journal of applied Physiology* **58**, 785-790 (1985).

29 Anversa, P., Ricci, R. & Olivetti, G. Quantitative structural analysis of the myocardium during physiologic growth and induced cardiac hypertrophy: a review. *Journal of the American College of Cardiology* **7**, 1140-1149 (1986).
30 Pelliccia, A., Maron, B. J., Spataro, A., Proschan, M. A. & Spirito, P. The upper limit of physiologic cardiac hypertrophy in highly trained elite athletes. *New England Journal of Medicine* **324**, 295-301 (1991).
31 Schannwell, C. M. *et al.* Left ventricular hypertrophy and diastolic dysfunction in healthy pregnant women. *Cardiology* **97**, 73-78 (2002).
32 Ro, A. & Frishman, W. H. Peripartum cardiomyopathy. *Cardiology in review* **14**, 35-42 (2006).
33 Bollen, I. A., Van Deel, E. D., Kuster, D. W. & Van Der Velden, J. Peripartum cardiomyopathy and dilated cardiomyopathy: different at heart. *Frontiers in physiology* **5**, 531 (2015).
34 Schiattarella, G. G. & Hill, J. A. Inhibition of Hypertrophy Is a Good Therapeutic Strategy in Ventricular Pressure Overload. *Circulation* **131**, 1435-1447, doi:doi:10.1161/CIRCULATIONAHA.115.013894 (2015).
35 Jones, D. W. *et al.* Partnering to reduce risks and improve cardiovascular outcomes: American Heart Association initiatives in action for consumers and patients. *Circulation* **119**, 340-350 (2009).
36 Stanley, W. C., Lopaschuk, G. D. & McCormack, J. G. Regulation of energy substrate metabolism in the diabetic heart. *Cardiovascular research* **34**, 25-33 (1997).
37 Perrino, C. *et al.* Intermittent pressure overload triggers hypertrophy-independent cardiac dysfunction and vascular rarefaction. *The Journal of clinical investigation* **116**, 1547-1560 (2006).
38 Shapiro, L. Physiological left ventricular hypertrophy. *Heart* **52**, 130-135 (1984).
39 Maron, B. J., Pelliccia, A., Spataro, A. & Granata, M. Reduction in left ventricular wall thickness after deconditioning in highly trained Olympic athletes. *Heart* **69**, 125-128 (1993).
40 Pelliccia, A. *et al.* Long-term clinical consequences of intense, uninterrupted endurance training in Olympic athletes. *Journal of the American College of Cardiology* **55**, 1619-1625 (2010).
41 Pelliccia, A. *et al.* Remodeling of left ventricular hypertrophy in elite athletes after long-term deconditioning. *Circulation* **105**, 944-949 (2002).
42 Ingwall, J. S. *ATP and the Heart*. Vol. 11 (Springer Science & Business Media, 2002).
43 Suga, H. Ventricular energetics. *Physiological reviews* **70**, 247-277 (1990).
44 Montaigne, D. *et al.* Myocardial contractile dysfunction is associated with impaired mitochondrial function and dynamics in type 2 diabetic but not in obese patients. *Circulation* **130**, 554-564 (2014).
45 Barton, G. P., de Lange, W. J., Ralphe, J. C., Aiken, J. & Diffee, G. Linking metabolic and contractile dysfunction in aged cardiac myocytes. *Physiological reports* **5** (2017).
46 Rosca, M. G., Tandler, B. & Hoppel, C. L. Mitochondria in cardiac hypertrophy and heart failure. *Journal of molecular and cellular cardiology* **55**, 31-41 (2013).
47 Burgoyne, J. R., Mongue-Din, H., Eaton, P. & Shah, A. M. Redox signaling in cardiac physiology and pathology. *Circulation research* **111**, 1091-1106 (2012).
48 Dai, D.-F. *et al.* Mitochondrial oxidative stress mediates angiotensin II–induced cardiac hypertrophy and Gαq overexpression–induced heart failure. *Circulation research* **108**, 837-846 (2011).
49 Gowans, Graeme J. & Hardie, D. G. AMPK: a cellular energy sensor primarily regulated by AMP. *Biochemical Society Transactions* **42**, 71-75, doi:10.1042/bst20130244 (2014).
50 Emerling, B. M. *et al.* Hypoxic activation of AMPK is dependent on mitochondrial ROS but independent of an increase in AMP/ATP ratio. *Free radical biology & medicine* **46**, 1386-1391, doi:10.1016/j.freeradbiomed.2009.02.019 (2009).
51 Beauloye, C., Bertrand, L., Horman, S. & Hue, L. AMPK activation, a preventive therapeutic target in the transition from cardiac injury to heart failure. *Cardiovascular research* **90**, 224-233 (2011).
52 Law, P.-Y. & Loh, H. H. Regulation of opioid receptor activities. *Journal of Pharmacology and Experimental Therapeutics* **289**, 607-624 (1999).
53 Pasternak, G. W. Multiple opiate receptors: deja vu all over again. *Neuropharmacology* **47**, 312-323 (2004).
54 Pradhan, A. A., Smith, M. L., Kieffer, B. L. & Evans, C. J. Ligand-directed signalling within the opioid receptor family. *British journal of pharmacology* **167**, 960-969 (2012).
55 Hodavance, S. Y., Gareri, C., Torok, R. D. & Rockman, H. A. G protein-coupled receptor biased agonism. *Journal of cardiovascular pharmacology* **67**, 193 (2016).
56 Campbell, A. P. & Smrcka, A. V. Targeting G protein-coupled receptor signalling by blocking G proteins. *Nature Reviews Drug Discovery* **17**, 789 (2018).
57 Zadina, J. E., Hackler, L., Ge, L.-J. & Kastin, A. J. A potent and selective endogenous agonist for the μ-opiate receptor. *Nature* **386**, 499 (1997).
58 Hojo, M. *et al.* μ-Opioid receptor forms a functional heterodimer with cannabinoid CB1 receptor: electrophysiological and FRET assay analysis. *Journal of pharmacological sciences* **108**, 308-319 (2008).
59 Waldhoer, M., Bartlett, S. E. & Whistler, J. L. Opioid receptors. *Annual review of biochemistry* **73**, 953-990 (2004).
60 Ananthan, S. in *Drug Addiction* 367-380 (Springer, 2008).
61 Zhang, S., Yekkirala, A., Tang, Y. & Portoghese, P. S. A bivalent ligand (KMN-21) antagonist for μ/κ heterodimeric opioid receptors. *Bioorganic & medicinal chemistry letters* **19**, 6978-6980 (2009).

62 Headrick, J. P., See Hoe, L. E., Du Toit, E. F. & Peart, J. N. Opioid receptors and cardioprotection – 'opioidergic conditioning' of the heart. *British Journal of Pharmacology* **172**, 2026-2050, doi:https://doi.org/10.1111/bph.13042 (2015).
63 Chang, M. C.-K. *et al.* Myocardial and peripheral concentrations of β-endorphin before and following myocardial ischemia and reperfusion during coronary angioplasty. *Japanese heart journal* **45**, 365-371 (2004).
64 Zöllner, C. & Stein, C. in *analgesia* 31-63 (Springer, 2006).
65 Santos, R. D. S. & Galdino, G. Endogenous systems involved in exercise-induced analgesia. *JPP* **1**, 01 (2018).
66 Jonsdottir, I., Hoffmann, P. & Thorèn, P. Physical exercise, endogenous opioids and immune function. *Acta physiologica scandinavica. Supplementum* **640**, 47-50 (1997).
67 Kraemer, W. J. *et al.* Effects of different heavy-resistance exercise protocols on plasma beta-endorphin concentrations. *Journal of Applied Physiology* **74**, 450-459 (1993).
68 DuPont, W. H. *et al.* The effects of different exercise training modalities on plasma proenkephalin Peptide F in women. *Peptides* **91**, 26-32 (2017).
69 Arida, R. M. *et al.* Differential effects of exercise on brain opioid receptor binding and activation in rats. *Journal of neurochemistry* **132**, 206-217 (2015).
70 Leal, A. K., Yamauchi, K., Kim, J., Ruiz-Velasco, V. & Kaufman, M. P. Peripheral δ-opioid receptors attenuate the exercise pressor reflex. *American Journal of Physiology-Heart and Circulatory Physiology* **305**, H1246-H1255 (2013).
71 Dickson, E. W. *et al.* Exercise enhances myocardial ischemic tolerance via an opioid receptor-dependent mechanism. *American Journal of Physiology-Heart and Circulatory Physiology* **294**, H402-H408 (2008).
72 Borges, J. P. *et al.* Delta opioid receptors: the link between exercise and cardioprotection. *PLoS One* **9**, e113541 (2014).
73 Tong, G. *et al.* Kappa-opioid agonist u50, 488h-mediated protection against heart failure following myocardial ischemia/reperfusion: dual roles of heme oxygenase-1. *Cellular Physiology and Biochemistry* **39**, 2158-2172 (2016).
74 Tong, G. *et al.* U50, 488H postconditioning reduces apoptosis after myocardial ischemia and reperfusion. *Life sciences* **88**, 31-38 (2011).
75 Butelman, E. R. *et al.* Kappa-opioid receptor binding populations in rhesus monkey brain: relationship to an assay of thermal antinociception. *Journal of Pharmacology and Experimental Therapeutics* **285**, 595-601 (1998).
76 Schultz, J. E., Hsu, A. K. & Gross, G. J. Ischemic preconditioning in the intact rat heart is mediated by delta1- but not mu- or kappa-opioid receptors. *Circulation* **97**, 1282-1289, doi:10.1161/01.cir.97.13.1282 (1998).
77 Kim, H. S. *et al.* Remifentanil protects myocardium through activation of anti-apoptotic pathways of survival in ischemia-reperfused rat heart. *Physiological research* **59**, 347-356 (2010).
78 Lessa, M. A. & Tibiriçá, E. Pharmacologic evidence for the involvement of central and peripheral opioid receptors in the cardioprotective effects of fentanyl. *Anesth Analg* **103**, 815-821, doi:10.1213/01.ane.0000237284.30817.f6 (2006).
79 Peart, J. N., Patel, H. H. & Gross, G. J. δ-Opioid receptor activation mimics ischemic preconditioning in the canine heart. *Journal of cardiovascular pharmacology* **42**, 78-81 (2003).
80 Estrada, J. A. *et al.* δ-Opioid receptor (DOR) signaling and reactive oxygen species (ROS) mediate intermittent hypoxia induced protection of canine myocardium. *Basic research in cardiology* **111**, 17 (2016).
81 Gross, E. R., Hsu, A. K. & Gross, G. J. Acute methadone treatment reduces myocardial infarct size via the δ-opioid receptor in rats during reperfusion. *Anesthesia and analgesia* **109**, 1395 (2009).
82 Gross, E. R., Peart, J. N., Hsu, A. K., Auchampach, J. A. & Gross, G. J. Extending the cardioprotective window using a novel δ-opioid agonist fentanyl isothiocyanate via the PI3-kinase pathway. *American Journal of Physiology-Heart and Circulatory Physiology* **288**, H2744-H2749 (2005).
83 Wang, G., Wang, H., Yang, Y. & Wong, T. M. κ-Opioid receptor stimulation inhibits growth of neonatal rat ventricular myocytes. *European journal of pharmacology* **498**, 53-58 (2004).
84 Lu, M. *et al.* The function of calcineurin and ERK1/2 signal in the antihypertrophic effects of κ-opioid receptor stimulation on myocardial hypertrophy induced by isoprenaline. *Die Pharmazie-An International Journal of Pharmaceutical Sciences* **67**, 182-186 (2012).
85 Yin, W. *et al.* Stimulation of κ-opioid receptor reduces isoprenaline-induced cardiac hypertrophy and fibrosis. *European journal of pharmacology* **607**, 135-142 (2009).
86 Jaiswal, A., Kumar, S., Seth, S., Dinda, A. K. & Maulik, S. K. Effect of U50, 488H, a κ-opioid receptor agonist on myocardial α-and β-myosin heavy chain expression and oxidative stress associated with isoproterenol-induced cardiac hypertrophy in rat. *Molecular and cellular biochemistry* **345**, 231-240 (2010).
87 Zhang, Q.-Y. *et al.* Antiarrhythmic effect mediated by κ-opioid receptor is associated with Cx43 stabilization. *Critical care medicine* **38**, 2365-2376 (2010).
88 Lin, J. *et al.* κ-Opioid receptor stimulation modulates TLR4/NF-κB signaling in the rat heart subjected to ischemia-reperfusion. *Cytokine* **61**, 842-848, doi:10.1016/j.cyto.2013.01.002 (2013).
89 Stark, R., Grzelak, M. & Hadfield, J. RNA sequencing: the teenage years. *Nature reviews. Genetics* **20**, 631-656, doi:10.1038/s41576-019-0150-2 (2019).

90 Chen, L. *et al.* Prediction and analysis of essential genes using the enrichments of gene ontology and KEGG pathways. *PLoS One* **12**, e0184129, doi:10.1371/journal.pone.0184129 (2017).
91 Ashburner, M. *et al.* Gene Ontology: tool for the unification of biology. *Nature Genetics* **25**, 25-29, doi:10.1038/75556 (2000).
92 Rockman, H. A., Wachhorst, S. P., Mao, L. & Ross Jr, J. ANG II receptor blockade prevents ventricular hypertrophy and ANF gene expression with pressure overload in mice. *American Journal of Physiology-Heart and Circulatory Physiology* **266**, H2468-H2475 (1994).
93 Merino, D. *et al.* Experimental modelling of cardiac pressure overload hypertrophy: Modified technique for precise, reproducible, safe and easy aortic arch banding-debanding in mice. *Scientific reports* **8**, 3167 (2018).
94 Reichert, K. *et al.* Murine Left Anterior Descending (LAD) Coronary Artery Ligation: An Improved and Simplified Model for Myocardial Infarction. *Journal of visualized experiments : JoVE*, doi:10.3791/55353 (2017).
95 Tarnavski, O. in *Cardiovascular Genomics* 115-137 (Springer, 2009).
96 Deussen, D. *Effects of opioid receptor agonist therapy on pressure overload induced cardiac hypertrophy and heart failure* Master of Science thesis, Maastricht University, (2013).
97 Rottman, J. N., Ni, G. & Brown, M. Echocardiographic evaluation of ventricular function in mice. *Echocardiography* **24**, 83-89 (2007).
98 Langmead, B. & Salzberg, S. L. Fast gapped-read alignment with Bowtie 2. *Nature methods* **9**, 357 (2012).
99 Li, B. & Dewey, C. N. RSEM: accurate transcript quantification from RNA-Seq data with or without a reference genome. *BMC bioinformatics* **12**, 323 (2011).
100 Robinson, M. D., McCarthy, D. J. & Smyth, G. K. edgeR: a Bioconductor package for differential expression analysis of digital gene expression data. *Bioinformatics* **26**, 139-140 (2010).
101 Young, M. D., Wakefield, M. J., Smyth, G. K. & Oshlack, A. Gene ontology analysis for RNA-seq: accounting for selection bias. *Genome biology* **11**, R14 (2010).
102 Xie, C. *et al.* KOBAS 2.0: a web server for annotation and identification of enriched pathways and diseases. *Nucleic acids research* **39**, W316-W322 (2011).
103 Rhee, S., Wood, V., Dolinski, K. & Draghici, S. Use and misuse of the gene ontology annotations. *Nature Reviews Genetics* **9**, 509-515 (2008).
104 Li, W. Volcano plots in analyzing differential expressions with mRNA microarrays. *Journal of bioinformatics and computational biology* **10**, 1231003, doi:10.1142/s0219720012310038 (2012).
105 Gehlenborg, N. & Wong, B. Heat maps. *Nature Methods* **9**, 213-213, doi:10.1038/nmeth.1902 (2012).
106 Weeks, K. L., Bernardo, B. C., Ooi, J. Y., Patterson, N. L. & McMullen, J. R. in *Exercise for Cardiovascular Disease Prevention and Treatment* 187-210 (Springer, 2017).
107 Samarel, A. M. Focal adhesion signaling in heart failure. *Pflügers Archiv-European Journal of Physiology* **466**, 1101-1111 (2014).
108 Hermans, K. C., Daskalopoulos, E. P. & Blankesteijn, W. M. Interventions in Wnt signaling as a novel therapeutic approach to improve myocardial infarct healing. *Fibrogenesis & tissue repair* **5**, 16 (2012).
109 Dawson, K., Aflaki, M. & Nattel, S. Role of the Wnt-Frizzled system in cardiac pathophysiology: a rapidly developing, poorly understood area with enormous potential. *The Journal of physiology* **591**, 1409-1432 (2013).
110 Cingolani, O. H. Cardiac hypertrophy and the Wnt/Frizzled pathway. *Hypertension* **49**, 427-428, doi:10.1161/01.HYP.0000255947.79237.61 (2007).
111 Blankesteijn, W. M., van de Schans, V. A., ter Horst, P. & Smits, J. F. The Wnt/frizzled/GSK-3 beta pathway: a novel therapeutic target for cardiac hypertrophy. *Trends Pharmacol Sci* **29**, 175-180, doi:10.1016/j.tips.2008.01.003 (2008).
112 Ai, Z., Fischer, A., Spray, D. C., Brown, A. M. & Fishman, G. I. Wnt-1 regulation of connexin43 in cardiac myocytes. *The Journal of clinical investigation* **105**, 161-171 (2000).
113 Fukami, K., Yamagishi, S.-i. & Okuda, S. Role of AGEs-RAGE system in cardiovascular disease. *Current pharmaceutical design* **20**, 2395-2402 (2014).
114 Kong, S. W. *et al.* Genetic expression profiles during physiological and pathological cardiac hypertrophy and heart failure in rats. *Physiological genomics* **21**, 34-42 (2005).
115 Strøm, C. C. *et al.* Expression profiling reveals differences in metabolic gene expression between exercise-induced cardiac effects and maladaptive cardiac hypertrophy. *The FEBS journal* **272**, 2684-2695 (2005).
116 Neri Serneri, G. G. *et al.* Increased cardiac sympathetic activity and insulin-like growth factor-I formation are associated with physiological hypertrophy in athletes. *Circulation research* **89**, 977-982 (2001).
117 Cambronero, F. *et al.* Biomarkers of pathophysiology in hypertrophic cardiomyopathy: implications for clinical management and prognosis. *European heart journal* **30**, 139-151 (2009).
118 Iemitsu, M. *et al.* Physiological and pathological cardiac hypertrophy induce different molecular phenotypes in the rat. *American Journal of Physiology-Regulatory, Integrative and Comparative Physiology* **281**, R2029-R2036 (2001).

119 McMullen, J. R. & Jennings, G. L. Differences between pathological and physiological cardiac hypertrophy: novel therapeutic strategies to treat heart failure. *Clinical and Experimental Pharmacology and Physiology* **34**, 255-262 (2007).
120 Menon, S. C. *et al.* Diastolic dysfunction and its histopathological correlation in obstructive hypertrophic cardiomyopathy in children and adolescents. *Journal of the American Society of Echocardiography* **22**, 1327-1334 (2009).
121 Wang, K. *et al.* κ-opioid receptor activation promotes mitochondrial fusion and enhances myocardial resistance to ischemia and reperfusion injury via STAT3-OPA1 pathway. *Eur J Pharmacol* **874**, 172987, doi:10.1016/j.ejphar.2020.172987 (2020).
122 Bosch-Marce, M. *et al.* Effects of aging and hypoxia-inducible factor-1 activity on angiogenic cell mobilization and recovery of perfusion after limb ischemia. *Circulation research* **101**, 1310-1318 (2007).
123 Eleuteri, E. *et al.* Prognostic value of angiopoietin-2 in patients with chronic heart failure. *International journal of cardiology* **212**, 364-368 (2016).
124 Sano, M. *et al.* p53-induced inhibition of Hif-1 causes cardiac dysfunction during pressure overload. *Nature* **446**, 444 (2007).
125 Wei, H. *et al.* Endothelial expression of hypoxia-inducible factor 1 protects the murine heart and aorta from pressure overload by suppression of TGF-β signaling. *Proceedings of the National Academy of Sciences* **109**, E841-E850 (2012).
126 Babcock, J. *et al.* Mechanism Governing Human Kappa-Opioid Receptor Expression under Desferrioxamine-Induced Hypoxic Mimic Condition in Neuronal NMB Cells. *International journal of molecular sciences* **18**, 211 (2017).
127 Maeder, M. T., Khammy, O., dos Remedios, C. & Kaye, D. M. Myocardial and systemic iron depletion in heart failure: implications for anemia accompanying heart failure. *Journal of the American College of Cardiology* **58**, 474-480 (2011).
128 Semenza, G. L. Hypoxia-inducible factor 1: regulator of mitochondrial metabolism and mediator of ischemic preconditioning. *Biochimica et Biophysica Acta (BBA)-Molecular Cell Research* **1813**, 1263-1268 (2011).
129 Rane, S. *et al.* Downregulation of miR-199a derepresses hypoxia-inducible factor-1α and Sirtuin 1 and recapitulates hypoxia preconditioning in cardiac myocytes. *Circulation research* **104**, 879-886 (2009).
130 Li, Y. *et al.* Heterodimerization of human apelin and kappa opioid receptors: roles in signal transduction. *Cell Signal* **24**, 991-1001, doi:10.1016/j.cellsig.2011.12.012 (2012).
131 Rostamzadeh, F. *et al.* Heterodimerization of apelin and opioid receptors and cardiac inotropic and lusitropic effects of apelin in 2K1C hypertension: Role of pERK1/2 and PKC. *Life sciences* **191**, 24-33 (2017).
132 Chen, M. M. *et al.* Novel role for the potent endogenous inotrope apelin in human cardiac dysfunction. *Circulation* **108**, 1432-1439 (2003).
133 Yeganeh-Hajahmadi, M., Najafipour, H., Farzaneh, F., Esmaeili-Mahani, S. & Joukar, S. Effect of apelin on cardiac contractility in acute reno-vascular hypertension: The role of apelin receptor and kappa opioid receptor heterodimerization. *Iranian journal of basic medical sciences* **21**, 1305 (2018).
134 Zhong, J.-C. *et al.* Apelin modulates aortic vascular tone via endothelial nitric oxide synthase phosphorylation pathway in diabetic mice. *Cardiovascular research* **74**, 388-395 (2007).
135 Zhang, J. *et al.* Apelin/APJ signaling promotes hypoxia-induced proliferation of endothelial progenitor cells via phosphoinositide-3 kinase/Akt signaling. *Molecular medicine reports* **12**, 3829-3834 (2015).
136 Zhang, J. *et al.* Exercise training promotes expression of apelin and APJ of cardiovascular tissues in spontaneously hypertensive rats. *Life sciences* **79**, 1153-1159 (2006).
137 Rostamzadeh, F., Najafipour, H., Yeganeh-Hajahmadi, M. & Joukar, S. Opioid receptors mediate inotropic and depressor effects of apelin in rats with 2K1C-induced chronic renovascular hypertension. *Clinical and Experimental Pharmacology and Physiology* **45**, 187-197 (2018).
138 Vinel, C. *et al.* The exerkine apelin reverses age-associated sarcopenia. *Nature medicine* **24**, 1360 (2018).
139 Fridolfsson, H. N. *et al.* Mitochondria-localized caveolin in adaptation to cellular stress and injury. *The FASEB Journal* **26**, 4637-4649 (2012).
140 Wang, J. *et al.* Cardioprotective trafficking of caveolin to mitochondria is Gi-protein dependent. *Anesthesiology: The Journal of the American Society of Anesthesiologists* **121**, 538-548 (2014).
141 Treskatsch, S. *et al.* Upregulation of the kappa opioidergic system in left ventricular rat myocardium in response to volume overload: adaptive changes of the cardiac kappa opioid system in heart failure. *Pharmacological research* **102**, 33-41 (2015).
142 Cai, Z. *et al.* Hearts from rodents exposed to intermittent hypoxia or erythropoietin are protected against ischemia-reperfusion injury. *Circulation* **108**, 79-85, doi:10.1161/01.CIR.0000078635.89229.8A (2003).
143 Foussal, C. *et al.* Activation of catalase by apelin prevents oxidative stress-linked cardiac hypertrophy. *FEBS Lett* **584**, 2363-2370, doi:10.1016/j.febslet.2010.04.025 (2010).
144 Tempel, D. *et al.* Apelin enhances cardiac neovascularization after myocardial infarction by recruiting aplnr+ circulating cells. *Circ Res* **111**, 585-598, doi:10.1161/CIRCRESAHA.111.262097 (2012).

145 Lakkisto, P. *et al.* Heme oxygenase-1 and carbon monoxide promote neovascularization after myocardial infarction by modulating the expression of HIF-1alpha, SDF-1alpha and VEGF-B. *Eur J Pharmacol* **635**, 156-164, doi:10.1016/j.ejphar.2010.02.050 (2010).
146 Mughal, A. & O'Rourke, S. T. Vascular effects of apelin: Mechanisms and therapeutic potential. *Pharmacol Ther* **190**, 139-147, doi:10.1016/j.pharmthera.2018.05.013 (2018).
147 Kim, Y. M. *et al.* Hypoxia-inducible factor-1alpha in pulmonary artery smooth muscle cells lowers vascular tone by decreasing myosin light chain phosphorylation. *Circ Res* **112**, 1230-1233, doi:10.1161/CIRCRESAHA.112.300646 (2013).
148 Ceylan-Isik, A. F. *et al.* Apelin administration ameliorates high fat diet-induced cardiac hypertrophy and contractile dysfunction. *J Mol Cell Cardiol* **63**, 4-13, doi:10.1016/j.yjmcc.2013.07.002 (2013).
149 Shohet, R. V. & Garcia, J. A. Keeping the engine primed: HIF factors as key regulators of cardiac metabolism and angiogenesis during ischemia. *J Mol Med (Berl)* **85**, 1309-1315, doi:10.1007/s00109-007-0279-x (2007).
150 Nakamoto, H., Oh, T., Shimamura, M., Iida, E. & Moritake, S. Nalfurafine hydrochloride for refractory pruritus in peritoneal dialysis patients: a phase III, multi-institutional, non-controlled, open-label trial. *Renal Replacement Therapy* **3**, 51 (2017).
151 Sunwoo, S. *et al.* Post-marketing surveillance study of the safety and efficacy of sildenafil prescribed in primary care to erectile dysfunction patients. *International journal of impotence research* **17**, 71 (2005).
152 Inui, S. Nalfurafine hydrochloride to treat pruritus: a review. *Clinical, cosmetic and investigational dermatology* **8**, 249 (2015).
153 Patel, H. H. *et al.* Protection of adult rat cardiac myocytes from ischemic cell death: role of caveolar microdomains and δ-opioid receptors. *American Journal of Physiology-Heart and Circulatory Physiology* **291**, H344-H350 (2006).
154 Du, J. *et al.* A decision analysis model for KEGG pathway analysis. *BMC bioinformatics* **17**, 407 (2016).
155 Barabasi, A.-L. & Oltvai, Z. N. Network biology: understanding the cell's functional organization. *Nature reviews genetics* **5**, 101 (2004).
156 Messing, K. & Mager Stellman, J. Sex, gender and women's occupational health: the importance of considering mechanism. *Environ Res* **101**, 149-162, doi:10.1016/j.envres.2005.03.015 (2006).
157 Soldin, O. P. & Mattison, D. R. Sex differences in pharmacokinetics and pharmacodynamics. *Clin Pharmacokinet* **48**, 143-157, doi:10.2165/00003088-200948030-00001 (2009).
158 Clayton, J. A. & Collins, F. S. Policy: NIH to balance sex in cell and animal studies. *Nature* **509**, 282-283, doi:10.1038/509282a (2014).
159 Parekh, A., Fadiran, E. O., Uhl, K. & Throckmorton, D. C. Adverse effects in women: implications for drug development and regulatory policies. *Expert Rev Clin Pharmacol* **4**, 453-466, doi:10.1586/ecp.11.29 (2011).

10. List of abbreviations

ACE - angiotensin converting enzyme
ADP - adenosine diphosphate
AET - aortic ejection time
AMPK - Adenosine monophosphate activated protein kinase
Angpt – angiopoietin
ANOVA - Analysis of variance
ANP - atrial natriuretic peptide
APLN - apelin
APJ - apelin receptor
ATP - adenosine triphosphate
BNP - B-type natriuretic peptide
bp - base pair
bpm - beats per minute
Ca^{2+} - calcium
cDNA - complementary DNA
CHF -chronic heart failure
CVD - cardiovascular disease
Cx43 - connexin43 / Gap junction alpha-1 protein
DOR - delta opioid receptor
DORA - delta opioid receptor agonist
ECHO - echocardiography
ECM - extracellular matrix
EF - ejection fraction
EGF - epidermal growth factor
EGFR - epidermal growth factor receptor
EU - European Union
FA - fatty acid
FIT - fentanyl isothiocyanate
FS - fractional shortening
GPCR - G protein-coupled receptor
GO - Gene Ontology Consortium
h - hour
HE - hematoxylin and eosin
HF - heart failure
HFmrEF - heart failure with mildly reduced ejection fraction
HFpEF - heart failure with preserved ejection fraction

HFrEF - heart failure with reduced ejection fraction
HIF - hypoxia induced factor
HO-1 - heme-oxygenase-1
HW - heart weight
ICD - intercalated disc
IGF - insulin growth factor
IHC - immunohistochemistry
IHD - ischemic heart disease
IPC - ischemic preconditioning
iTAC - intermitted transverse aortic constriction
KEGG - Kyoto Encyclopedia at Genes and Genomes
KOR - kappa opioid receptor
KORA - kappa opioid receptor agonist
LAD - left anterior descending coronary artery
log - logarithm
LV - left ventricle
LVIDd - left ventricular internal dimension in diastole
LVIDs - left ventricular internal dimension in systole
LVH - left ventricular hypertrophy
LVPWd - left ventricular end diastolic posterior wall dimension
LVSD - left ventricular systolic dysfunction
IVSd - inter ventricular septal end diastolic dimension
M - molar
MAPK - mitogen-activated protein kinase
MHC - myosin heavy chain
mM- millimolar
MI - myocardial infarct
min - minute
mg - milligram
mm - millimeter
MOR - mu opioid receptor
mRNA - messenger ribonucleic acid
mTOR - mammalian target of rapamycin
n - number
NOP - nociceptin/ orphanin receptor
nor-BNI - nor-binaltorphimine
NYHA - New York Heart Association

ORL - opioid receptor-like orphan receptor
OR - opioid receptor
ORA - opioid receptor agonist
p – p-value
PCR - polymerase chain reaction
PCr - phosphocreatine
PDYN - pro-dynorphin
PENK - pro-enkephalin
PI3K - phosphoinositide 3-kinase
POMC - pro-opiomelanocortin
PPCM - peripartum cardiomyopathy
q-PCR - quantitative polymerase chain reaction
RAAS - renin–angiotensin–aldosterone system
RNA - ribonucleic acid
RNA-seq - RNA or cDNA sequencing
ROS - reactive oxygen species
RT - room temperature
S6K - ribosomal S6 kinases
SD - standard deviation
SEM - standard error of the means
SHR - spontaneous hypertensive rat
TAC - transverse aortic constriction
TEM - transmission electron microscopy
TGF-β - transforming growth factor-β
TL - tibia length
tx - drug treatment
U50 - (±)-U-50488 hydrochloride
UCSD - University of California, San Diego
v. - version
Vcf - mean velocity of circumferential fiber shortening
Vcl - vinculin
VEGF - vascular endothelial growth factor
wk - week
wnt - wnt signaling pathway

11. Acknowledgement / Danksagung

Zuerst möchte ich herzlichst Univ.-Prof. Dr. med. Reinhard Lorenz, vom Institut für Prophylaxe und Epidemiologie der Kreislaufkrankheiten (IPEK), für sein Engagement und seine Unterstützung dieses externen Promotionsvorhabens danken.

Professor Hemal Patel gebührt besonderer Dank, dafür dass er mich in seine Arbeitsgruppe aufgenommen hat, mir dieses spannende Projekt zugetraut hat und mir stets zur Seite gestanden hat.

Mit Ihrer großen Erfahrung und Ihrer Begeisterung beim Vermitteln von Wissen und Techniken, hat Dr. med. univ. Alice Zemljic-Harpf im Labor und besonders bei der Echokardiografie, einen großen Beitrag an dieser Arbeit geleistet.

Der deutschen Herzstiftung danke ich für die finanzielle Unterstützung während des Aufenthaltes an der Universität San Diego.

Bei der Ausarbeitung des vorliegenden Schriftstückes bedanke ich mich bei Tobias Hübner für seine Hilfe bei der grafischen Gestaltung der Abbildungen zur Herzhypertrophie, und Elena Kopp für ihr Lektorat und ihre Unterstützung.

Zum Abschluss gilt großer Dank meiner Familie, die mich während meines gesamten Lebens- und Bildungsweges stets mit allen Mitteln unterstützt hat.

Ich erkläre hiermit an Eides statt,
dass ich die vorliegende Dissertation mit dem Titel

A microscopic and transcriptome sequencing approach to protective mechanisms of opioid receptor stimulation in murine pressure overload induced heart failure

selbständig verfasst, mich außer der angegebenen keiner weiteren Hilfsmittel bedient und alle Erkenntnisse, die aus dem Schrifttum ganz oder annähernd übernommen sind, als solche kenntlich gemacht und nach ihrer Herkunft unter Bezeichnung der Fundstelle einzeln nachgewiesen habe.

Ich erkläre des Weiteren, dass die hier vorgelegte Dissertation nicht in gleicher oder in ähnlicher Form bei einer anderen Stelle zur Erlangung eines akademischen Grades eingereicht wurde.

Daniel Nils Deußen München, den 21.10.2021